

Staufen Recruitment into Stress Granules Does Not Affect Early mRNA Transport in Oligodendrocytes

María G. Thomas,^{*†} Leandro J. Martínez Tosar,^{*†} Mariela Loschi,^{*}
Juana M. Pasquini,[‡] Jorge Correale,[§] Stefan Kindler,^{||} Graciela L. Boccaccio^{*¶}

^{*}Fundación Instituto Leloir, IIB Facultad de Ciencias Exactas y Naturales, University of Buenos Aires, IIBBA-CONICET, Buenos Aires, Argentina; [†]Instituto de Química y Fisicoquímica Biológica, Facultad de Farmacia y Bioquímica, University of Buenos Aires, CONICET, Buenos Aires, Argentina; [§]Department of Neurology, Instituto de Investigaciones Neurológicas Raúl Carrea (FLENI), Buenos Aires, Argentina; and ^{||}Institute for Cell Biochemistry and Clinical Neurobiology, Center for Molecular Neurobiology, University Hospital Hamburg-Eppendorf, University of Hamburg, Hamburg, Germany

Submitted June 24, 2004; Revised September 29, 2004; Accepted October 20, 2004

Monitoring Editor: Peter Walter

Staufen is a conserved double-stranded RNA-binding protein required for mRNA localization in *Drosophila* oocytes and embryos. The mammalian homologues Staufen 1 and Staufen 2 have been implicated in dendritic RNA targeting in neurons. Here we show that in rodent oligodendrocytes, these two proteins are present in two independent sets of RNA granules located at the distal myelinating processes. A third kind of RNA granules lacks Staufen and contains major myelin mRNAs. Myelin Staufen granules associate with microfilaments and microtubules, and their subcellular distribution is affected by polysome-disrupting drugs. Under oxidative stress, both Staufen 1 and Staufen 2 are recruited into stress granules (SGs), which are stress-induced organelles containing transiently silenced messengers. Staufen SGs contain the poly(A)-binding protein (PABP), the RNA-binding proteins HuR and TIAR, and small but not large ribosomal subunits. Staufen recruitment into perinuclear SGs is paralleled by a similar change in the overall localization of polyadenylated RNA. Under the same conditions, the distribution of recently transcribed and exported mRNAs is not affected. Our results indicate that Staufen 1 and Staufen 2 are novel and ubiquitous SG components and suggest that Staufen RNPs are involved in repositioning of most polysomal mRNAs, but not of recently synthesized transcripts, during the stress response.

INTRODUCTION

From the early steps of mRNA transport to the latest events of degradation, cytoplasmic RNA granules are highly relevant to the physiology of mRNA, including silencing and activation (reviewed in Wickens and Goldstrohm, 2003). Granules packaging targeted mRNAs appear in oligodendrocytes and other polarized vertebrate cells as dense structures, containing also ribosomes and with an average diameter of 1 μm (Barbarese *et al.*, 1995; Barry *et al.*, 1996; Ainger *et al.*, 1997; Knowles and Kosik, 1997; Carson *et al.*, 2001; Krichevsky and Kosik, 2001). A different type of RNA granules known as stress granules (SGs) appears transiently upon induction of cellular stress. SGs are large ribonucleoparticles (RNPs) and are thought to be in dynamic equilib-

rium with translating polysomes (Kedersha *et al.*, 2000, 2002; Anderson and Kedersha, 2002).

The double-stranded RNA-binding protein Staufen emerges as a relatively ubiquitous RNA granule-forming factor (Ferrandon *et al.*, 1994, 1997; Duchaine *et al.*, 2000; Kiebler and DesGroseillers, 2000; Micklem *et al.*, 2000). This protein was initially described in *Drosophila* oocytes, where it is found in granules involved in microtubule-dependent localization of maternal mRNAs to define the anterior-posterior axis of the embryo (Lasko, 1999; Kloc *et al.*, 2002). Staufen is recruited into granules upon its interaction with *bicoid* mRNA 3'UTR sequences that mediate targeting of the messenger, and it is strictly required for the formation of these granules (Ferrandon *et al.*, 1994, 1997). Likewise, the positioning of *oskar* mRNA at the oocyte posterior pole involves the formation of Staufen-containing granular structures known as polar bodies (Lasko, 1999; Kloc *et al.*, 2002). Staufen also participates in actin-dependent segregation of *prospero* mRNA during asymmetric division of embryonic CNS cells (reviewed in Lasko, 1999; Kiebler and DesGroseillers, 2000; Kloc *et al.*, 2002). Moreover, *Drosophila* Staufen is essential for long-term memory acquisition, a phenomenon known to require mRNA targeting followed by local translation at the synapse (Dubnau *et al.*, 2003).

Two homologous genes, Staufen 1 and Staufen 2, were reported in mammals and amphibians (Kiebler and DesGroseillers, 2000; Monshausen *et al.*, 2001; Tang *et al.*, 2001; Kress *et al.*, 2004; Yoon and Mowry, 2004). Evidence sup-

Article published online ahead of print. Mol. Biol. Cell 10.1091/mbc.E04-06-0516. Article and publication date are available at www.molbiolcell.org/cgi/doi/10.1091/mbc.E04-06-0516.

[†] These authors contributed equally to this work.

[¶] Corresponding author. E-mail address: gboccaccio@leloir.org.ar.

Abbreviations used: RNP, ribonucleoparticle; MBPs, myelin basic proteins; PABP, poly(A)-binding protein; SGs, stress granules; RBD, double-stranded RNA-binding domain; ER, endoplasmic reticulum; PDI, protein disulphide isomerase; DRB, 5,6-dichlobenzimidazole riboside; NMD, non-sense-mediated decay.

porting Staufen participation in mRNA localization in vertebrate neurons and oocytes is emerging. Motile RNA granules containing Staufen 1 and Barentsz—a protein partner of *Drosophila* Staufen also involved in mRNA transport—are present in the somatodendritic compartment (Kiebler *et al.*, 1999; Kohrmann *et al.*, 1999; Macchi *et al.*, 2003). Rat Staufen 1 binds to the dendrite targeting element (DTE) of MAP2 mRNA (Monshausen *et al.*, 2001) and, in addition, Staufen 1 RNPs isolated from brain and cortical neurons contain localized RNAs and associate to motor molecules (Krichevsky and Kosik, 2001; Ohashi *et al.*, 2002; Mallardo *et al.*, 2003; Kanai *et al.*, 2004). Furthermore, overexpression of a truncated form of Staufen 2 leads to a reduction of the dendritic RNA content (Tang *et al.*, 2001). Likewise, interference strategies in amphibian oocytes indicates that *Xenopus* Staufen 1 is involved in the late localization pathway to the vegetal pole (Kress *et al.*, 2004; Yoon and Mowry, 2004).

In this study, we investigated the distribution of Staufen 1 and Staufen 2 in rodent oligodendrocytes, where the extra-somatic translation of mRNAs is important during myelin biogenesis and repair (Brophy *et al.*, 1993; Carson *et al.*, 1998, 2001; Barbarese *et al.*, 1999). We show that Staufen 1, Staufen 2, and the major myelin-targeted mRNA, which encodes myelin basic protein (MBP), reside in three distinct subsets of cytoplasmic granules that are present in both, somata and cell processes. We found that in addition to normal granules, Staufen 1 and Staufen 2 are recruited into stress granules. However, the redistribution of these proteins into SGs does not interfere with the movement of recently transcribed RNAs toward the oligodendrocyte processes. Our results suggest a role for Staufen 1 and Staufen 2 RNPs in the relocation of polysomal mRNAs in response to different stimuli and—as an extreme example—their coalescence into perinuclear SGs upon oxidative stress.

MATERIALS AND METHODS

Primary Antibodies Against Staufen 1 and Staufen 2

Rabbit polyclonal (RLS1) and mouse polyclonal (MLS1) antisera were raised against a recombinant protein carrying the native RBD3 from murine Staufen 1 fused to lumazine synthase from *Brucella abortus* (Craig, Berguer, Armcart, Zylberman, Thomas, Martinez Tosar, Bulloj, Boccaccio, and Goldbaum unpublished results). For Staufen 2, an affinity-purified rabbit polyclonal anti-serum (336) was prepared against a rat N-terminal peptide including RBD1 and first RBD2 hemidomain. Isoform specificity of the RLS1 and 336 antisera was confirmed in cell lines overexpressing Staufen 2 or Staufen 1. Previously described rabbit antibodies anti-Staufen 1 were also used: 3326 antisera (Monshausen *et al.*, 2002) and two antisera kindly provided by J. Ortín and M. Kiebler (Kiebler *et al.*, 1999; Marion *et al.*, 1999).

Primary Oligodendrocyte Culture and Drug Treatment

Oligodendrocyte cultures were established from 1- to 4-d-old Sprague Dawley rat brains as previously described (McCarthy and deVellis, 1980), with minor modifications. Oligodendrocyte precursors were recovered from a primary culture by shaking, plated onto poly-L-lysine and incubated either in complete medium (Suzumura *et al.*, 1984; DMEM/Ham's F12 supplemented with 10% fetal bovine serum [FBS], 5 µg/ml streptomycin, 5 U/ml penicillin, and cytosine arabinoside as mitotic inhibitor when required), or in glial defined medium (GDM: DMEM/Ham's F12 supplemented with 2.4 mg/ml sodium bicarbonate, 3.58 mg/ml HEPES, 50 mg/ml transferrin, 5 mg/ml insulin, 5.2 ng/ml sodium selenite, 2.5 ng/ml biotin, 0.7 mg/ml hydrocortisone, 10 ng/ml triiodothyronine, 50 U/ml penicillin, 50 mg/ml streptomycin, 1% FBS, pH 7.4) to yield oligodendrocyte preparations virtually free of other cell types (Casaccia-Bonelli *et al.*, 1996). All chemicals for cell culture were purchased from Sigma. FBS was from Life Technologies (Rockville, MD). Stock solutions of puromycin and cycloheximide (Sigma, St. Louis, MO), 5,6-dichlorobenzimidazole riboside (DRB, ICN Biomedicals, Aurora, OH), NaAsO₂ (Merck, Rahway, NJ) and edeine (generous gift from Dr. I. Algranati) were diluted in conditioned medium before use.

Protein synthesis inhibition was evaluated as follows: ¹⁴C-labeled amino acids (0.02 µCi/well) were added 1 h after exposure to edeine, and the radioactivity incorporated into trichloroacetic acid (TCA) precipitate was measured 2 h later.

Cloning of Staufen 1 Splicing Variants

Murine brain Staufen 1 cDNA clones were obtained from 21-d-old animals by PCR cloning using the primers: 5'-TGCAAGCTTCTGGGAAGCAGCCA-GAAAG-3' and 5'-CCGTCTAGATGCAGCCATATCATGACAGGACT-3'. For semiquantitative RT-PCR analysis we used a pair of primers flanking the intron present in exon 9 (5'-TCAAGGACACCACCAAAG-3' and 5'-CAGGGTCTAGTGCAGG-3'). Serial dilutions of brain cDNA were analyzed. The relative intensities of the 94- (spliced) and 179-base pair (non-spliced) bands in ethidium bromide gels, and Southern blots were compared with that of standard reactions in which plasmids carrying spliced and nonspliced Staufen 1 cDNAs were used as templates at ratios 1:10, 1:100, and 1:1000.

Immunofluorescence

Cells were fixed at 37°C in 4% paraformaldehyde supplemented with 4% sucrose in phosphate-buffered saline (PBS), permeabilized, and blocked in 2% bovine serum albumin supplemented with 10% normal goat serum. Incubations with primary and secondary antibodies (Molecular Probes, Eugene, OR; Jackson ImmunoResearch Laboratories, West Grove, PA) were performed for 1 h at room temperature and followed by three washes in PBS containing

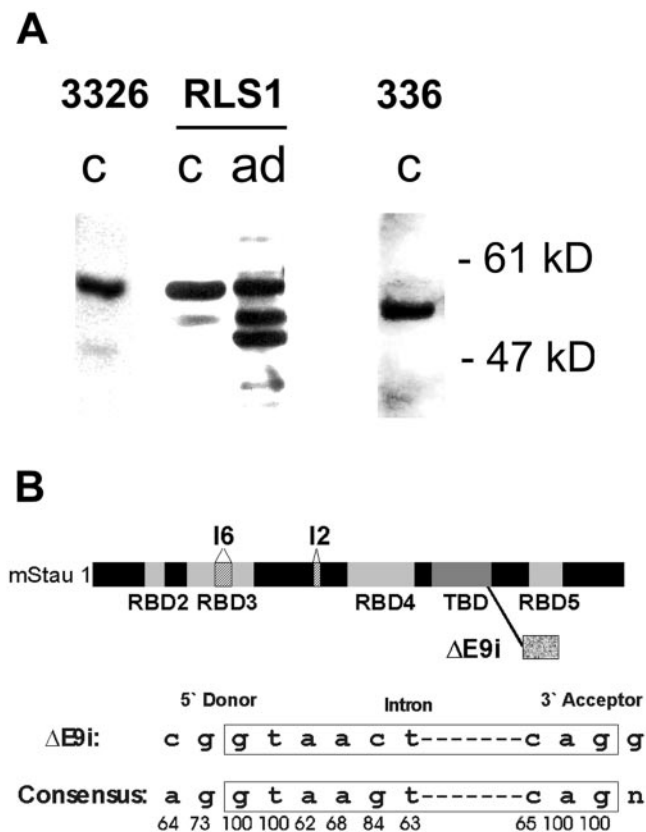


Figure 1. Expression of Staufen 1 and Staufen 2 in rat oligodendrocytes. (A) Western blot analysis of oligodendrocyte cytosolic extracts with 3326 (1:500) and RLS1 (1:10,000) antisera against Staufen 1 and the 336 antiserum (1:500) against Staufen 2. Extracts were incubated 16 h at 37°C (ad, autodigested) or prepared in the presence of protease inhibitors (c, control). The 49-kDa band includes a novel splicing variant named ΔE9i, as well as degradation products of the 55-kDa band. (B) Staufen 1 splicing variants isolated from mouse brain. An 85-base pair intron is spliced out from exon 9 in the ΔE9i Staufen 1 variant (Acc. No AY391773), which encodes a 49-kDa polypeptide. The variant I2 (Acc. No. AF395842) has 2 extra amino acids in the poorly conserved segment connecting RBD3 and RBD4 and corresponds to an alternative 3' acceptor site at exon VI. The Staufen 1 I6 was described previously (Monshausen *et al.*, 2001; Duchaine *et al.*, 2002). Numbers indicate the frequency of the consensus bases at the splice site. RBD, double-stranded RNA-binding domain; TBD, tubulin-binding domain.

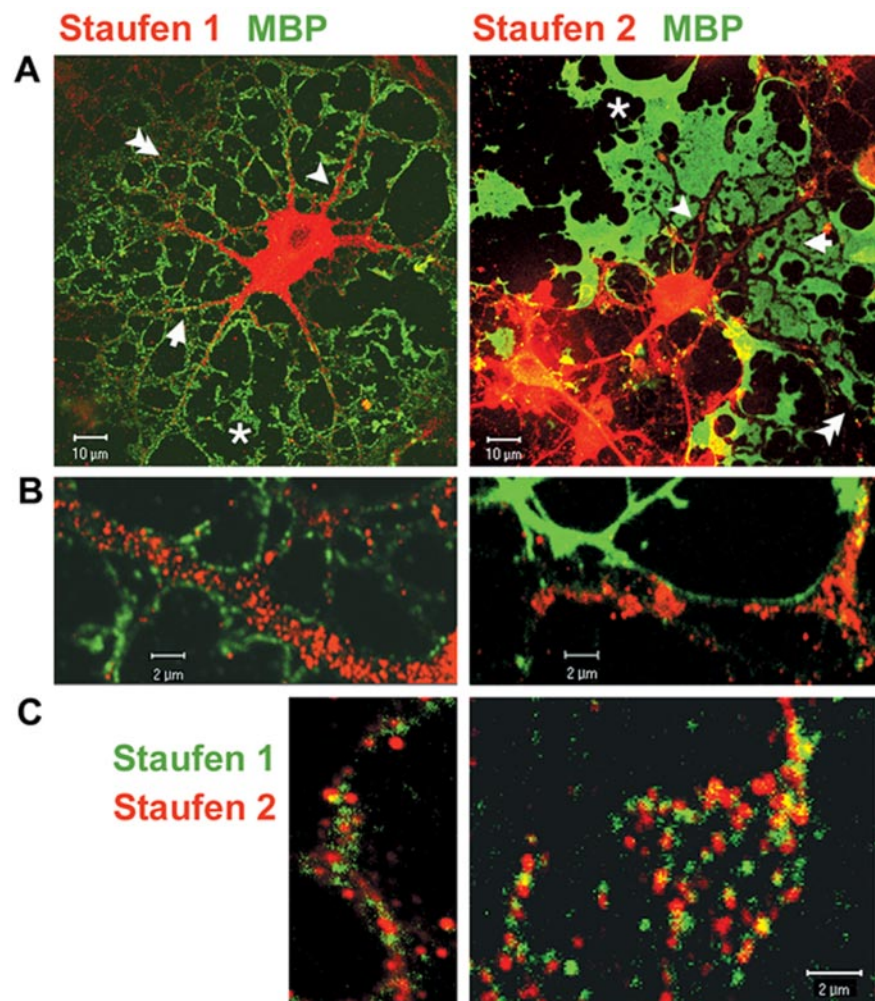


Figure 2. Staufen 1 and Staufen 2 form granules in mature rat oligodendrocytes. (A and B) Cells were immunostained for Staufen 1 or Staufen 2 (red, left and right, respectively) and for the oligodendrocyte membrane marker MBP (green). Staufen proteins form granules present in primary processes (arrowheads); secondary processes (arrows) and distal myelinating extensions (double arrowheads), and are excluded from the flattened myelin membrane extensions that are uniformly stained for MBP (asterisks). (B) Staufen 1 and Staufen 2 granules are ~500-nm size and are abundant at the distal myelin compartment. The same granular pattern was observed with different antibodies anti-Staufen 1. (C) Distal branches (left) and myelinating extension (right) of cells immunostained for Staufen 1 (MLS1, green) and Staufen 2 (336, red). Only a minor proportion of the granules were double-stained for both proteins.

0.05% Tween (PBST). Primary antibodies were diluted as follows: RLS1, 1:500; MLS1, 1:100; and 3326, 1:100. Anti-PAPB rabbit polyclonal antibody (kindly provided by Dr. Evita Mohr, University of Hamburg, Germany), 1:500; monoclonal antibodies anti-TIAR (BD Biosciences, San José, CA); Y10B against rRNA and anti-HuR (gifts from Dr. Joan Steitz, Yale University), 1:100; monoclonal antibodies against beta-tubulin (Sigma) and protein disulphide isomerase (PDI; StressGen, Victoria, British Columbia, Canada), 1:500. Alexa 546-labeled phalloidin (Molecular Probes) was used at 1:40. Cells were mounted in Mowiol 4–88 (Calbiochem, La Jolla, CA).

Fluorescent In Situ Hybridization (FISH) and Combined FISH-Immunofluorescence

Two different MBP cDNA fragments were cloned into pBlueScript II-KS (Stratagene, La Jolla, CA): 1) a 1911-base pair fragment isolated by PCR from rat brain cDNA using the primers: 5'-CAGCGACACGGATCCAAGTACTT-3' and 5'-AAAGCGGCCGCTACTGCAGCTGCCCTGTC-3'; and 2) a 660-base pair *Hind*III restriction fragment from rat MBP-14 (Staugaitis *et al.*, 1990). Antisense and sense digoxigenin-RNA probes were synthesized *in vitro* according to the manufacturer's protocol (Roche Diagnostics, Basel, Switzerland). Cells were fixed in 4% paraformaldehyde, 4% sucrose, 2 mM MgCl₂ in PBS for 15 min at 37°C, washed three times in 4% sucrose, PBS and UV cross-linked (CL program, GS Gene Linker, Bio-Rad, Hercules, CA). Cells were then permeabilized in 0.3% Triton X-100 in PBS for 5 min, washed with 2 mM MgCl₂ in PBS, and dried completely. After prehybridization in 50% formamide, 5× SSC, 0.2% SDS, 50 µg/ml heparin, 250 ng/ml salmon sperm DNA, and 250 µg/ml yeast tRNA (all from Sigma), overnight hybridization was performed at 55°C in the same solution supplemented with 100 µg/ml heparin and 100 ng/ml digoxigenin-riboprobe. After washing twice at room temperature with 1× SSC, 0.1% SDS, and twice at 50°C with 0.2× SSC, 0.1% SDS, blocking was performed with 1% Blocking Reagent (Boehringer Mannheim, Indianapolis, IN) in PBS. The probe signal was amplified in one or two steps with the following antibodies: biotinylated mouse antidiogoxin

(Sigma) or sheep antidiogoxigenin (Boehringer Mannheim) followed by biotinylated donkey anti-sheep (Jackson ImmunoResearch). Then, streptavidin coupled to Cy3 (Jackson ImmunoResearch) or Alexa 488 (Molecular Probes) was used. All incubations were for 2 h at room temperature and were followed by three washes in PBST. When FISH was combined with immunofluorescence (IF), the first antibody for the IF was either included in the antidiogoxin antibody solution or used after the biotinylated donkey anti-sheep. The secondary antibody for IF was always included in the streptavidin mix.

Colocalization by Confocal Imaging Analysis and Computer-assisted Simulations

Images were acquired in an LSM 510 or LSM 5 PASCAL confocal microscope (Carl Zeiss, Oberkochen, Germany). Proper equipment adjustment was ensured using 1-µm FocalCheck fluorescent microspheres (Molecular Probes). Colocalization analysis was performed in representative regions of interest by counting single and double-stained granules with the "Manual Tag" tool of the Image ProPlus software (Media Cybernetics, Silver Springs, MD). To estimate the random colocalization frequency in the micrographs, we ran a computer-simulation representing two independently distributed pools of particles, similarly to previously described approaches (Jacobs *et al.*, 1999). Data of granule area and population sizes to be loaded into the simulation program were acquired from the confocal micrographs. Briefly, random coordinates were assigned to single particles in an Excel spreadsheet (Microsoft, Redmond, WA) to represent their positions in a two-dimensional area and distances between granule centers were calculated for each pair of particles. A distance smaller than particle radius was scored as a colocalization event. Each run of the simulation considered ~100 particles of the most abundant species. The random colocalization frequency in each subcellular region was averaged from 30 runs of the simulation.

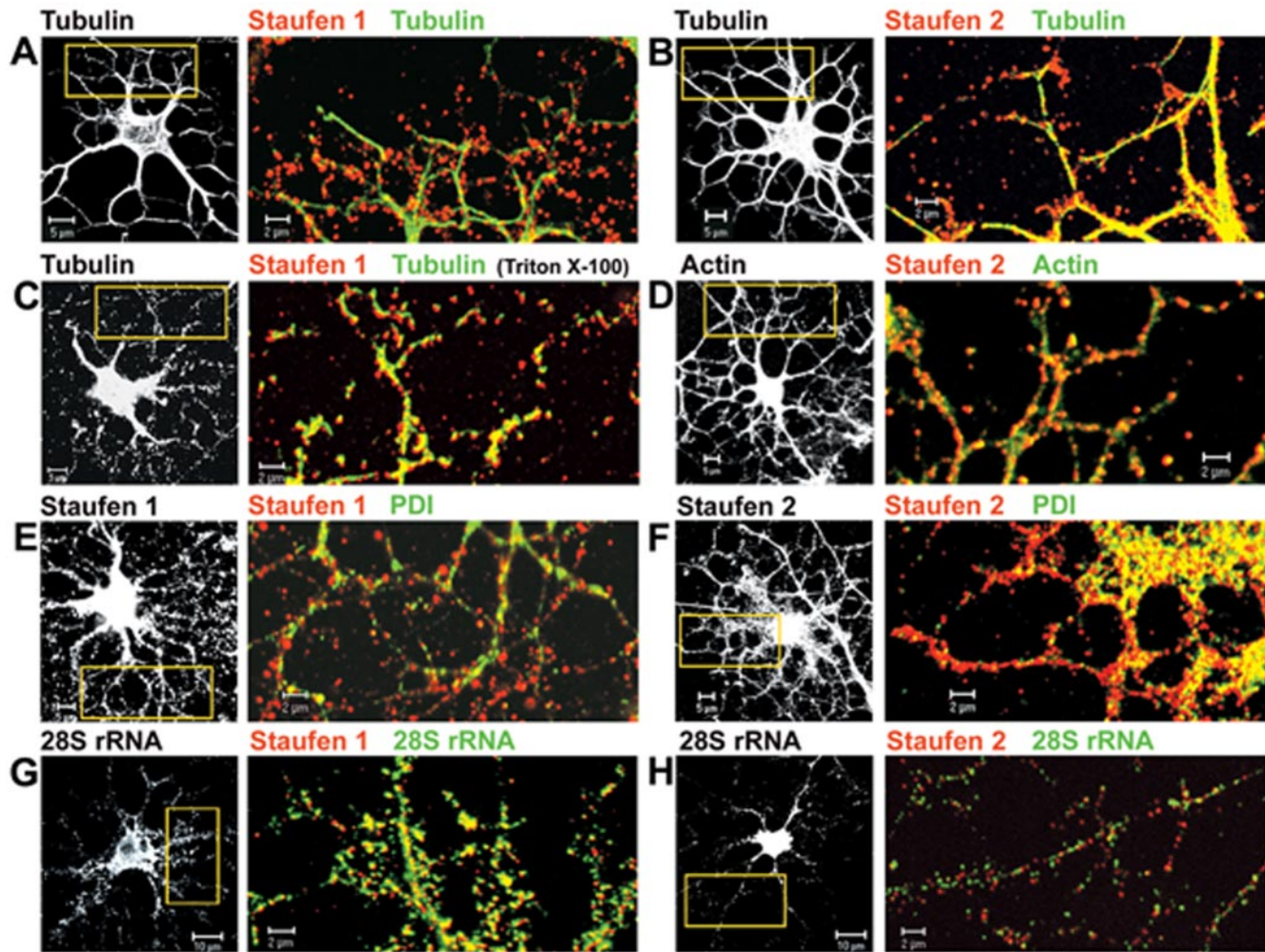


Figure 3. Association of Staufen granules with cytoskeleton, ER, and ribosomal subunits. Yellow boxes indicate the position of the enlarged fields shown in color. Representative immunostainings for Staufen 1 (left panels, red) and Staufen 2 (right panels, red) are shown. Tubulin (A–C), actin (D), the ER marker PDI (E and F), and large ribosomal subunits (G and H) are in green. (A–D) Staufen 1 and Staufen 2 granules are associated to microtubules as well as to microfilaments in the distal regions. Staufen 1 (C) and Staufen 2 (unpublished data) remained associated to microtubules after a brief extraction of living cells with Triton X-100. (E and F) Staufen 1 and Staufen 2 granules are often found in the vicinity of ER membranes in the proximal tubulin-rich regions and not associated to them in the distal branches. (G and H) Most Staufen 1 granules contain ribosomal subunits, whereas Staufen 2 colocalize to a minor degree. In both cases, ribosome-containing granules free of Staufen proteins are also present.

Myelin and Cytoskeleton Preparation and RNase Treatment

Brains from 3-wk-old Sprague Dawley rats were homogenized in 0.8 M sucrose, CSK buffer (CSKB: 25 mM KCl, 1 mM HEPES, pH 6.8, 1 mM EGTA, 5 mM MgCl₂) containing the protease inhibitors 4-(2-aminoethyl)benzenesulfonyl fluoride (AEBSF), pepstatinA, E-64, bestatin, leupeptin, and aprotinin (Sigma). Homogenates were separated by centrifugation in discontinuous 0.8–0.25 M sucrose gradients at 220,000 × g for 1 h at 4°C, and a myelin-enriched fraction was recovered from the interphase. A cytoskeleton fraction was isolated by treatment of myelin extracts with 5% Triton X-100, 0.25 M sucrose in CSKB for 15 min at 37°C, followed by centrifugation as above. Myelin cytoskeleton or oligodendrocyte total extracts containing 0.1% Triton X-100 and 0.25 M sucrose in CSKB were incubated in the presence or absence of 300 µg/ml RNase A (Amersham Pharmacia, Uppsala, Sweden), for 15 min at 37°C with gentle shaking. After centrifugation at 9300 × g for 10 min at 4°C, equivalent amounts of the soluble and pellet fractions were analyzed by Western blot.

Sedimentation Velocity Centrifugation

Cytosolic extracts from primary cultures grown in GDM were prepared in 0.5% Triton X-100, 0.25 M sucrose in CSKB. For protein analysis cytosolic extracts containing 0.5–1 mg of protein (determined by the Bicinchoninic Acid

Protein Assay Kit, Sigma) were loaded onto continuous 13-ml sucrose gradients (20–60% wt/vol in CSKB) and centrifuged at 220,000 × g for either 2 or 4 h. When indicated, cells were previously exposed 30 min to 0.250 mg/ml cycloheximide. The polysomal profile was monitored by absorbance at 260 nm. Protein from 1-ml fractions was precipitated using 20 µg of lysozyme as carrier and subjected to Western blot analysis.

For analysis of tritiated RNA, cytosolic extracts prepared in 0.5% Triton X-100, 0.25 M sucrose in CSKB containing 0.02 mg/ml cycloheximide were loaded onto 10–30% wt/vol sucrose gradients and centrifuged 4 h. Radioactivity incorporated in TCA-precipitated material was determined in a liquid scintillation counter.

Western Blotting

After precipitation in chloroform/methanol (1:2), protein samples were resuspended in Laemmli sample-buffer, separated by SDS-PAGE, and electro-transferred to Immobilon-P PVDF membranes (Millipore, Bedford, MA). The following primary antibodies were used: RLS1 (diluted 1:5000–1:10,000), 3326 (1:500), 336 (1:500), antitubulin (1:1000), and rabbit anti-S6 (Cell Signaling, Beverly, MA, 1:1000). Detection was performed with peroxidase-coupled antibodies (Sigma) followed by chemoluminescence with LumiGlo reagents (Cell Signaling).

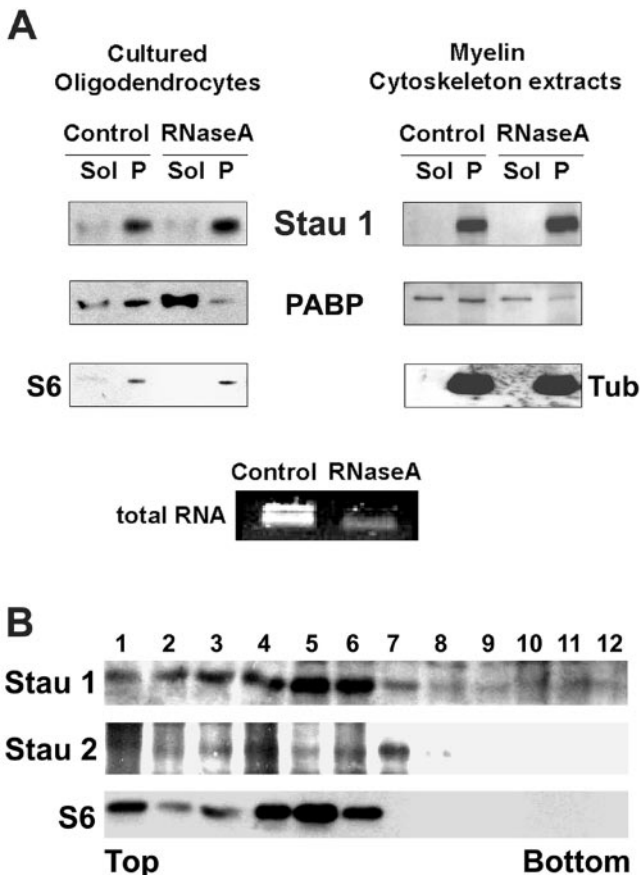


Figure 4. RNase A sensitivity and sedimentation velocity analysis of Staufen 1 complexes. (A) Oligodendrocyte and myelin cytoskeleton extracts were treated with RNase A in the presence of Triton X-100 and then separated in a soluble fraction (Sol) and a pellet (P) enriched in ribosomes (S6) and tubulin (Tub). Staufen 1 is retained in the pellet, and RNA breakdown does not affect its distribution. In contrast, PABP is completely released into the soluble fraction upon RNA digestion. Bottom: RNA was analyzed in an EtBr-agarose gel. (B) Cytosolic extracts from GDM cultures exposed to cycloheximide were analyzed by centrifugation (2 h) in a sedimentation gradient. Staufen 1 and Staufen 2 comigrate with average-sized polyosomes.

Metabolic Radiolabeling of RNA

Primary oligodendrocytes differentiated for 2–3 wk in vitro were incubated in medium containing 1 μ M (50 μ Ci/ml) [5,6-³H]uridine (NET 367, New England Nuclear, Boston, MA, or TRK410, Amersham) for 1 h, as described for neurons (Kleinman *et al.*, 1993). After addition of 1 mM unlabeled uridine, cells were fixed and dehydrated by treatment with 25–100% ethanol serial solutions. Coverslips were glued to microscope slides (cells facing upwards) and coated with Kodak NTB2 autoradiography emulsion (Eastman-Kodak, Rochester, NY). After exposure for 7 d in a desiccating dark chamber, they were developed using Kodak Dektol solutions. Bright field micrographs (400 \times) were acquired in an Olympus BX60 microscope (Lake Success, NY) coupled to a CoolSnap-Pro digital camera (Media Cybernetics) and analyzed with the Image-Pro Plus software. Signal intensity was measured in 1- μ m-thick annular sections of increasing radii centered in the cell nucleus. Background signal in equivalent rings from a field with no cells in the same sample was subtracted. Intensity relative to the whole-cell labeling was plotted against distance from the nucleus. For treatment with DRB, the inhibitor was present during the pulse and chase period at 70 μ M. For treatment with edeine, cells were chased in the presence of 0.1 mM of the drug.

Tritiated RNA was separated in formaldehyde/formamide 1% agarose gels. After separation, radioactivity was measured in 0.25-cm gel slices from the origin to the running front.

RESULTS

Expression of Staufen 1 and Staufen 2 in Oligodendrocytes

We analyzed the expression of Staufen 1 and Staufen 2 in oligodendrocytes by Western blot of purified myelin and primary culture extracts. The presence of a major band of 55 kDa, which corresponds to the predicted mouse Staufen 1 molecular weight, was confirmed with several rabbit and a mouse polyclonal antibodies raised against Staufen 1 (Figure 1A; GenBank Acc. No. AF227200 and AF061942). In addition, we observed a minor band of 49 kDa, likely representing a novel splicing variant that we named Staufen Δ E9i (Figure 1B, Acc. No. AY391773). Sequence analysis of Staufen Δ E9i clones indicated that this transcript lacks an intron that is included in the splicing variants that were previously described. This leads to a +2 frameshift, rendering a transcript with a premature stop codon located 75 base pairs upstream to the last exon-exon junction. Messengers with this configuration are usually degraded by the cellular mechanism known as non-sense-mediated decay (NMD; reviewed in Maquat and Carmichael, 2001). Thus, we compared the relative abundance of mRNAs including or excluding this intron by semiquantitative RT-PCR analysis. We found that Δ E9i mRNA is 100 times less abundant than transcripts including the intron in the P21 mouse brain. This is in accordance with the low abundance of the encoded protein, which was subsequently not further analyzed.

The expression of Staufen 2 in oligodendrocytes was investigated using the affinity-purified rabbit polyclonal antibody 336. We observed a single 53-kDa band (Figure 1A), which is in accordance with the previously reported molecular weight for one of the three splicing variants described in rodents (Duchaine *et al.*, 2002).

Staufen 1 and Staufen 2 form Granules in Myelinating Processes

Immunofluorescence of primary rat oligodendrocytes indicated that both, Staufen 1 and Staufen 2 are present in granules of ~500 nm in diameter that are abundant in somata and cellular branches (Figure 2A). In myelinating processes, Staufen granules were found restricted to cytoplasmic channels and absent from the flattened myelin membrane extensions neatly mapped by MBP staining (Figure 2, A and B). Simultaneous detection of Staufen 1 and Staufen 2 revealed that the two isoforms preferentially reside in distinct granules (Figure 2C), being only a minor proportion double-stained for both proteins (15%).

We then investigated the association of Staufen molecules with the cytoskeleton and ER membranes, which participate in RNA localization and translation in several systems (Kloc *et al.*, 2002; López de Heredia and Jansen, 2003 and references therein). Staufen 1 and Staufen 2 granules were found associated with microtubules at the proximal processes (Figure 3, A–C) as well as with actin microfilaments in the most distal myelin regions (Figure 3D). Furthermore, Staufen 1 and Staufen 2 remained associated to microtubules after extraction of cytosolic components by treatment of living cells with Triton X-100 (Figure 3C and unpublished data). This selective partitioning was also confirmed by Western blot assays of myelin and oligodendrocyte extracts submitted to a similar treatment (Figure 4A). Visualization of the ER marker PDI showed that both Staufen 1 and Staufen 2 granules were frequently associated with ER membranes in the tubulin-rich oligodendrocyte processes (Figures 3, E and F). However, Staufen granules located at the most distal myelinating extensions—likely representing the granules linked to the microfilament system (Figure 3D)—were not

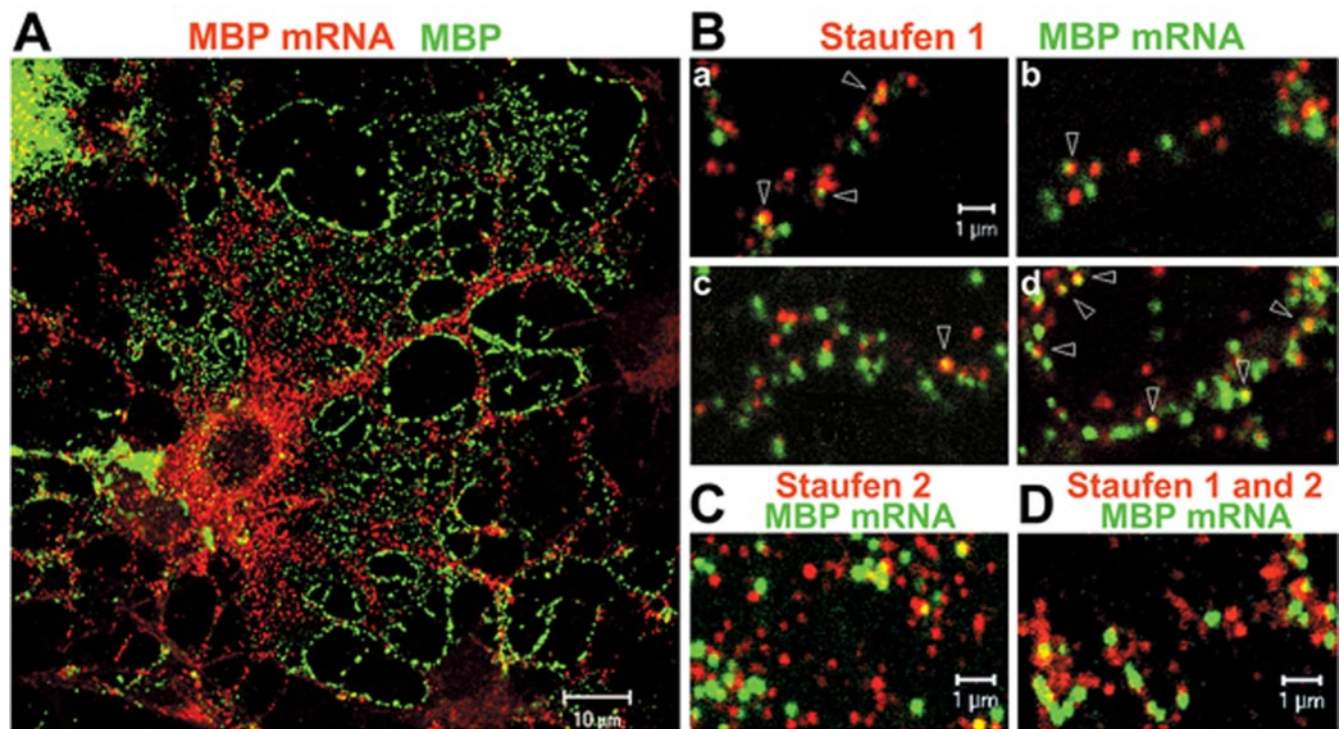


Figure 5. Staufen 1, Staufen 2, and MBP mRNAs reside in three different sets of granules. (A) Simultaneous FISH (red) and IF (green) for MBP. MBP mRNAs display a granular pattern in the perinuclear compartment, primary processes, and distal myelinating extensions. A PLP riboprobe yielded a coarsely granular pattern concentrated in the perinuclear cytoplasm, whereas no signal was observed with a sense MBP probe (unpublished data). (B) Simultaneous detection of Staufen 1 (red) and MBP mRNA (green) indicates no colocalization of these molecules in primary processes (a), secondary branches (b), branch interconnections (c), and distal myelinating extensions (d). A few double-stained granules resulting from random colocalization (see Table 1) are indicated by arrowheads. (C) The colocalization of Staufen 2 (red) and MBP mRNA (green) at the myelin membrane compartment is as well infrequent. (D) No significant colocalization is observed when Staufen 1 and Staufen 2 detected with the RLS1 and 336 antisera (both in red) were simultaneously visualized with MBP mRNAs (green).

associated with the scarce ER membranes present in this region (Figures 3, E and F). Double staining with the Y10B antibody revealed that most Staufen 1 and a fraction of Staufen 2 granules contain ribosomes (Figure 3, G and H).

Given that Staufen is a RNA-binding protein that forms granules containing ribosome subunits, we analyzed the sensitivity of these RNPs to RNA digestion. Cultured oligodendrocytes and myelin cytoskeleton extracts were treated with RNase A in the presence of Triton X-100 and subsequently separated into a pellet representing the cytoskeletal/polysomal fraction and a supernatant corresponding to the unbound crude fraction. The distribution of Staufen 1, of the poly(A) binding protein (PABP) and of the small ribosomal subunit marker S6 were analyzed by Western blot. In both, oligodendrocyte and myelin samples, Staufen 1 and S6 remained in the pellet fraction whereas PABP was completely released to the unbound fraction upon partial RNA digestion (Figure 4A). These results suggested the preferential interaction of Staufen 1 with microtubules or with RNase A-resistant ribosome subunits. We further investigated the nature of Staufen complexes by studying its association with polysomes. We performed sedimentation velocity analyses of cytosolic extracts obtained from highly pure oligodendrocyte cultures. Figure 4B shows that Staufen 1 and Staufen 2 comigrated with polysomes, clearly identified by the presence of S6 (see also Figure 6). As expected, tubulin and PDI were exclusively detected in the top fractions (unpublished data).

Altogether these results indicated that in oligodendrocytes, Staufen granules associate to both microfilaments and microtubules and that Staufen 1 and Staufen 2 associate to polysomes.

Staufen and MBP mRNAs Reside in Distinct Granule Populations

MBP mRNAs are the major transcripts localized at the myelinating processes (Gould *et al.*, 2000; Carson *et al.*, 2001). In accordance with previous data (reviewed in Barbarese *et al.*, 1999, Carson *et al.*, 2001), FISH analysis of MBP mRNAs showed that these transcripts reside in granules of uniform size (200–500 nm), present at the perinuclear compartment as well as at the primary and fine distal branches (Figure 5A). Although Staufen 1 and Staufen 2 were more abundant at the perinuclear cytoplasm (Figure 2; see also Kohrmann *et al.*, 1999), the size, density, and localization of MBP mRNA granules at the cell processes were remarkably similar to that of Staufen 1 and Staufen 2 granules. However, double staining for MBP mRNAs and Staufen 1 or Staufen 2 indicated that Staufen proteins do not colocalize with these major myelin transcripts (Figure 5, B and C). On average, the percentage of double-stained granules for Staufen 1 was <15%, with no significant difference in primary, secondary, and distal processes (Table 1). A similar analysis for Staufen 2 also indicated a reduced colocalization frequency (15%) with MBP mRNA-positive granules (Figure 5C). For comparison, MBP mRNA-PABP colocalization was analyzed,

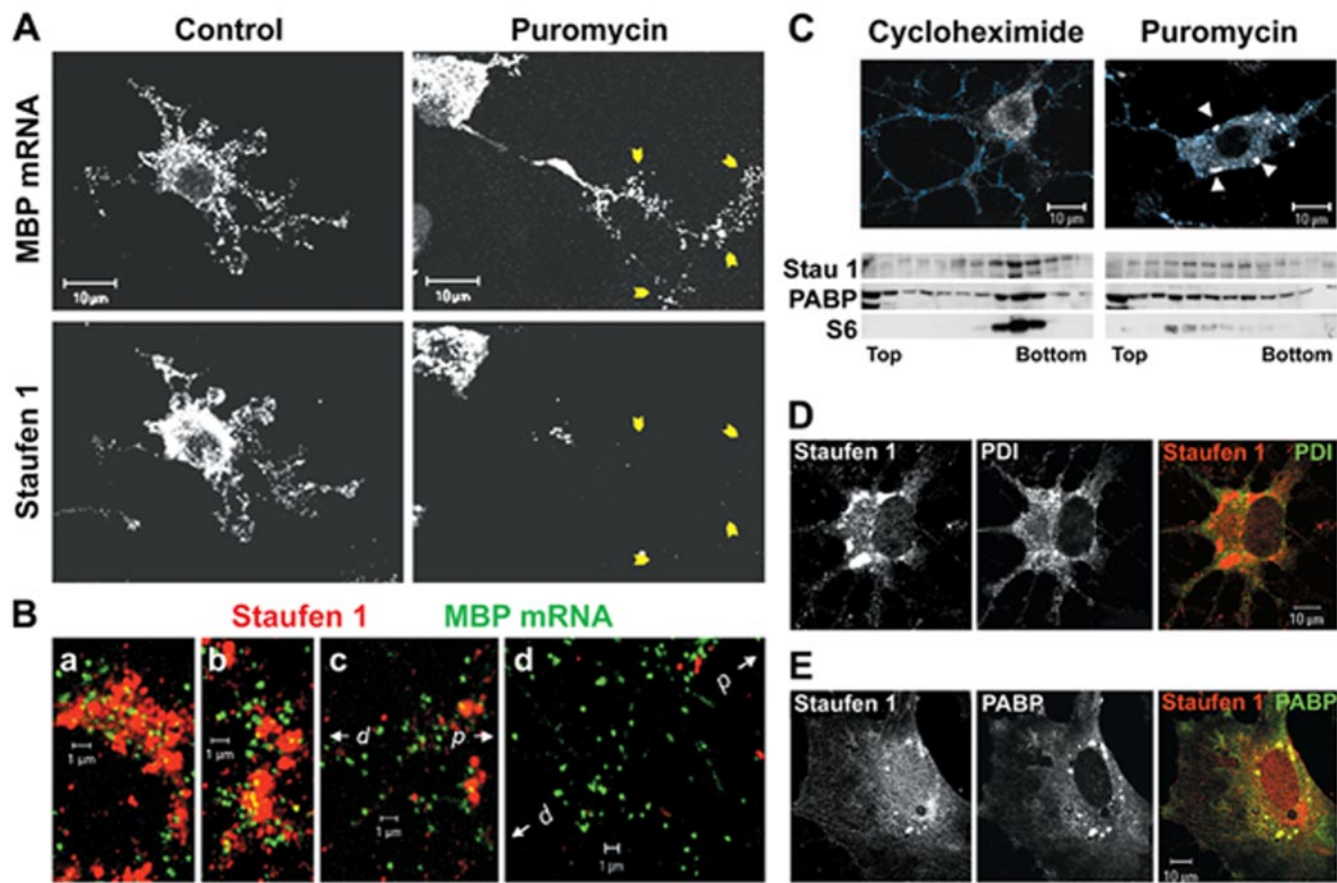


Figure 6. Staufen redistributes upon puromycin treatment. (A) MBP mRNA distribution remains unchanged, whereas the number of Staufen 1 granules at the distal processes is greatly reduced after 4-h treatment with 250 μ g/ml puromycin (arrowheads). (B) Staufen 1 granules (red) aggregate into large clusters in primary and secondary processes and branching points (a and b), and virtually disappear from the distal branches and membrane extensions (c and d, d, distal; p, proximal). The fine granular pattern of MBP mRNA (green) is retained. (C) Staufen 1 (right panel) and Staufen 2 (unpublished data) are recruited into perinuclear accretions after puromycin treatment, whereas cycloheximide (left panel) elicits no effect. IF for MBP is shown in light blue. Western blot: Staufen 1 sedimentation profile shifts together with S6 and PABP distributions, accompanying polysome disassembly. (D) Puromycin-induced Staufen 1 clusters do not include ER membranes, identified by PDI. An astrocyte is shown. (E) Puromycin-induced Staufen 1 clusters contain PABP. A primary fibroblast is depicted.

indicating that 60% of MBP mRNA granules contained this protein (Table 1). In addition, we confirmed that the antigenicity of Staufen molecules was not affected by the FISH procedure, as judged by signal intensity, abundance and size of the granules. Finally, in all cell regions, the

colocalization frequency observed experimentally matched the values predicted for a random distribution (Table 1). These results indicated that under steady-state conditions, Staufen granules do not include MBP mRNAs as a regular component and thus, we conclude that

Table 1. Staufen 1 and the major myelin-targeted mRNA display independent distributions

	MBP mRNA/Staufen 1	Staufen 1/MBP mRNA	MBP mRNA/PABP	Random colocalization ^a
Primary	11.5 ± 3.0	11.5 ± 3.9	56.5 ± 11.2 ^b	11.6 ± 5.2
Secondary	14.4 ± 5.1	15.3 ± 4.9	60.9 ± 9.5 ^b	11.05 ± 4.9
Distal	12.7 ± 3.7 ^b	15.6 ± 5.0	55.0 ± 9.7 ^b	19.6 ± 6.4

Colocalization is expressed as the percentage of double-stained granules relative to the total number of granules positive for a single marker in primary, secondary, or distal myelinating processes. An average of 20 optical fields was analyzed for each subcellular region, adding up ~900 granules of each kind per region. Staining with two different anti-Staufen 1 antibodies (RLS1, and 3326) and two different MBP mRNA riboprobes yielded consistent results indicating a low proportion of doubled-labeled granules.

^a As obtained by computer-assisted simulation of randomly distributed particles with size and abundance according to experimental observations (see Materials and Methods).

^b Significantly differs from values for a random colocalization in the same cellular region, according to a Student's *t* test (*p* < 0.01).

Staufen 1, Staufen 2, and the major myelin messengers reside in different RNA granules.

Staufen 1 and Staufen 2 Redistribute upon Polysome Disruption

Given that Staufen granules associate to polysomes, we investigated the integrity of Staufen granules upon polysome disruption by puromycin. We found that Staufen 1 and Staufen 2 granules dramatically redistributed after treatment. The number of Staufen 1 granules at distal cell extensions was greatly reduced (Figure 6A) and instead, Staufen 1 granules were found concentrated at proximal processes, branching points and somata (Figure 6B). On puromycin treatment, both Staufen 1 and Staufen 2 accumulated in the cell body in large discrete structures of 2–5-μm size (Figure 6C and unpublished data). For comparison, MBP mRNAs were simultaneously analyzed. We found that, in contrast with Staufen redistribution, the localization of these messengers remained largely unchanged (Figure 6A). The puromycin-induced Staufen redistribution was observed in ~60% of the cells in addition to oligodendrocytes, astrocytes, and fibroblasts (Figure 6, C–E). No effect was elicited by cycloheximide, a translation inhibitor that causes stabilization of polysomes (Figure 6C).

As normal Staufen granules were partially found in apposition with the ER and the cytoskeleton (Figure 3), we investigated if this association is affected by puromycin. Staining for PDI indicated that the ER morphology was not disrupted and, moreover, ER membranes were completely excluded from the Staufen 1 accretions (Figure 6D). We also observed that microfilaments and microtubules were not affected by the treatment (unpublished data). Altogether, these observations indicated that puromycin-induced Staufen redistribution was not accompanied by a similar change in ER or cytoskeleton remodeling.

The distribution of the general mRNA binding protein PABP was simultaneously analyzed. PABP is normally homogeneously distributed throughout the cytoplasm, and was recruited in the puromycin-induced Staufen clusters in all cell types (Figure 6E).

Staufen 1 and Staufen 2 Are Recruited into Stress Granules

It has been reported that polysome disruption upon cellular stress induces the accumulation of a number of RNA binding proteins and elements of the translational machinery, such as PABP, in perinuclear densities known as stress granules (SGs; Kedersha *et al.*, 2000, 2002; Anderson and Kedersha, 2002). SG formation is also observed upon exposure to polysome destabilizing drugs such as puromycin and inhibited by cycloheximide (Anderson and Kedersha, 2002). We hypothesized that the puromycin-induced Staufen accumulations represent stress granules and thus, we analyzed the Staufen distribution upon induction of oxidative stress by arsenite, a known SG-inducing factor. On exposure to 0.5 mM arsenite, Staufen 1 and Staufen 2 were recruited into large aggregates that were similar to the puromycin-induced structures and were also observed in every cell type present in the culture (left panels in Figures 7 and 8). Then, we investigated the presence of the RNA binding protein TIAR, a well-known marker of stress granules (Kedersha *et al.*, 2000; Anderson and Kedersha, 2002). We found that the arsenite-induced Staufen 1 and Staufen 2 clusters contained TIAR and moreover, all the SGs identified by TIAR included Staufen molecules (Figure 7, A–D). Interestingly, Staufen 1 and Staufen 2 colocalized in SGs (Figure 7E),

in contrast to their normal distribution in two nonoverlapping sets of granules.

We investigated the presence of general translation components, namely PABP and ribosomal subunits in Staufen SGs. As expected, arsenite-induced Staufen 1 stress granules contained PABP and small ribosomal subunits (Figure 8, A and B) as described for SGs (Kedersha *et al.*, 2002). Interestingly, the Y10B antibody did not stain Staufen SGs (Figure 8C), likely reflecting its stronger reactivity against large subunit rRNA (Lerner *et al.*, 1981; Gardon *et al.*, 1995) and in accordance with the absence of 60S subunits from SGs (Kedersha *et al.*, 2002). In addition, we observed that HuR, an RNA-binding protein frequently present in SGs (Gallouzi *et al.*, 2000) was also found in Staufen clusters (Figure 8D).

It is known that stress granules contain transcripts that are transiently silenced (Kedersha *et al.*, 2002). Consistently, we found that upon arsenite-induced stress, MBP mRNA partially coalesced into large perinuclear aggregates (Figure 8E, middle panels). However, as in normal conditions, stress-induced accumulations of Staufen 1 and MBP mRNA were mutually exclusive (Figure 8E).

All these observations indicated that Staufen 1 and Staufen 2 were simultaneously recruited into SGs upon puromycin or arsenite treatment. The redistribution of Staufen 1 and 2 upon stress was paralleled by a similar change in PABP localization, indicating that most polyadenylated RNAs were recruited into SGs containing Staufen.

Recruitment of Staufen into Stress Granules Does Not Affect the Cytoplasmic Transport of Newly Synthesized Transcripts

In oligodendrocytes, an active transport of mRNAs from the nuclear periphery to the distal myelinating extensions occurs (Carson *et al.*, 1998, 2001; Barbarese *et al.*, 1999). Given that Staufen molecules were reported to participate in cytoplasmic RNA transport in different cell systems, we sought to investigate the effect of Staufen recruitment into SGs on the movement of recently synthesized transcripts, immediately after their export from the cell nucleus.

Newly transcribed mRNAs were metabolically radiolabeled by a pulse with tritiated uridine and their subcellular localization was monitored at different chase times (*Materials and Methods*). We first ensured that the incorporated radioactivity was completely sensitive to RNase A. We also found that 70% of the radiolabeled RNA remained bound to magnetic oligodT beads (unpublished data). When total RNA was analyzed in denaturing agarose gels (Figure 9A), we found that a large proportion of radioactivity (87%) migrated between 5 and 0.5 kb, representing mRNAs and rRNAs. The ribosomal RNAs bands, which also include mRNAs, contained 45% of radioactivity. Thus, at least 42% of incorporated radioactivity corresponded to mRNAs. Furthermore, cytosolic extracts where separated by sedimentation velocity centrifugation and radioactivity distribution was evaluated along the gradient. We found that the first fractions, which correspond to mRNPs, contained 41% of total incorporated radioactivity. Peaks corresponding to ribosomal subunits (fraction 7–24) comprised 42% of radioactivity. Finally, 17% was recovered in the bottom fractions, where polysomes and large RNPs migrate (Figure 9A). Considering that rRNAs are ~50 times more abundant than polyadenylated RNA, the specific radioactivity of rRNA was 100 times lower than that of polyadenylated mRNAs. All this observations are in agreement with reported data, indicating that the synthesis rate of mRNA is higher than that of rRNA (Jackson *et al.*, 1998). As shown

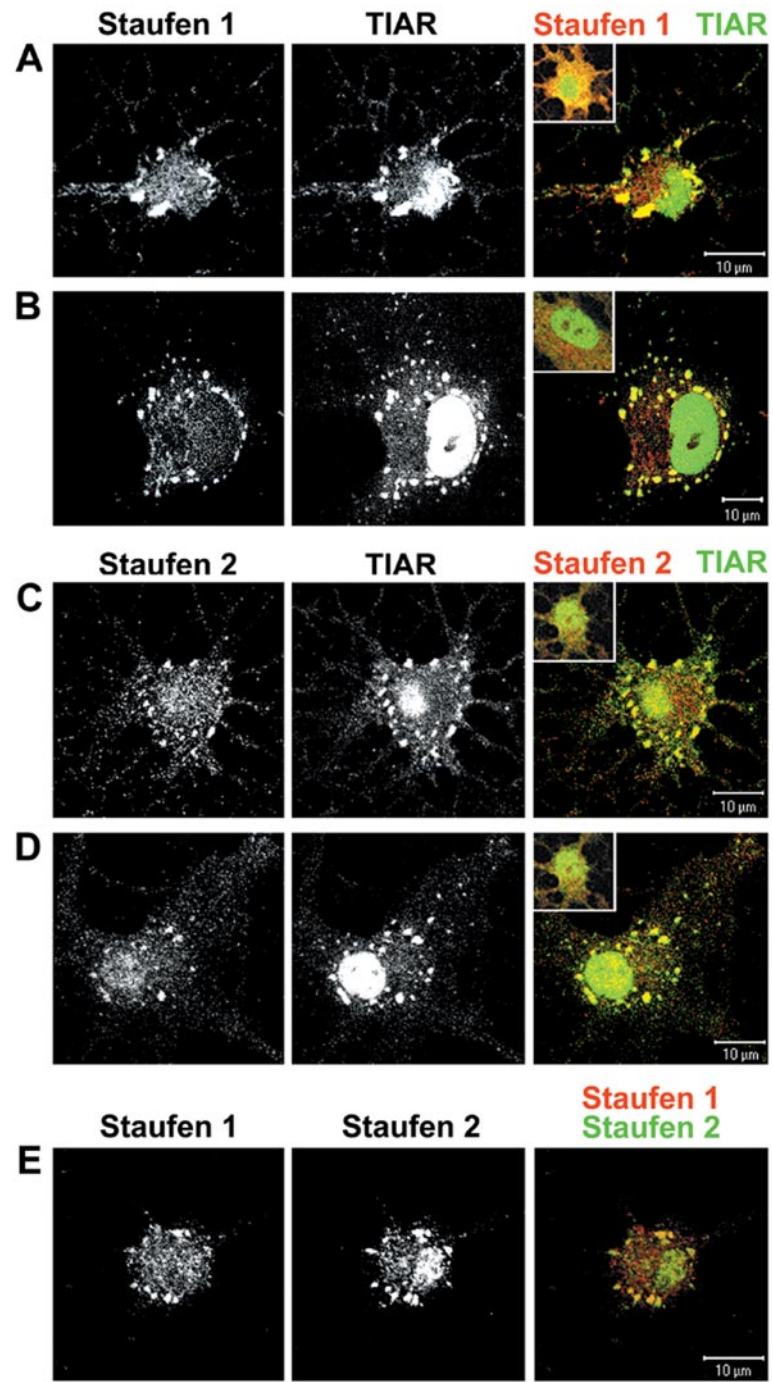


Figure 7. Oxidative stress induces the recruitment of Staufen 1 and Staufen 2 into stress granules (SGs). Staufen 1 (A and B) and Staufen 2 (C and D) form perinuclear aggregates after 1-h treatment with 0.5 mM arsenite. The SG-marker protein TIAR strictly colocalizes with Staufen accumulations. As previously described, TIAR was found restricted to the cell nucleus in normal conditions (A-D, insets). (E) Staufen 1 and Staufen 2 colocalizes in SGs. Representative oligodendrocytes (A, C, and E); primary fibroblasts (B) and astrocytes (D) are shown.

in Figure 9B, immediately after the pulse, tritiated mRNA molecules were restricted to the nucleus and perinuclear cytoplasm. After a 4-h chase, radiolabeled mRNAs reached the major cellular processes and 12 h later they were detected at the most distal branches (Figure 9B). After an overnight chase, the nucleus was almost free of radioactivity, whereas the intensity of the signal at the myelinating extensions remained high, likely reflecting the accumulation of very stable mRNAs in this region (Mathisen *et al.*, 1997).

For comparison, pulse-chase radiolabeling was performed in the presence of DRB, an RNA polymerase II-inhibitor that provokes the accumulation of truncated transcripts which

are not exported from the nucleus. As expected, the presence of DRB completely abrogated the signal in the cytoplasm (Figure 9C). A distribution profile of radiolabeled mRNAs was obtained by plotting incorporated radioactivity against distance from the cell center at different chase times (Figure 9D). The data indicated that mRNAs being transported to the cell processes moved at an average speed of 6 μm/h, a value comparable to that reported in neurons (10 μm/h, Kleinman *et al.*, 1993).

Next, we used this assay to study the effect of Staufen aggregation into SGs over mRNA transport to the cell processes. Because the induction of oxidative stress would deeply affect cellular metabolism and motor activity, we

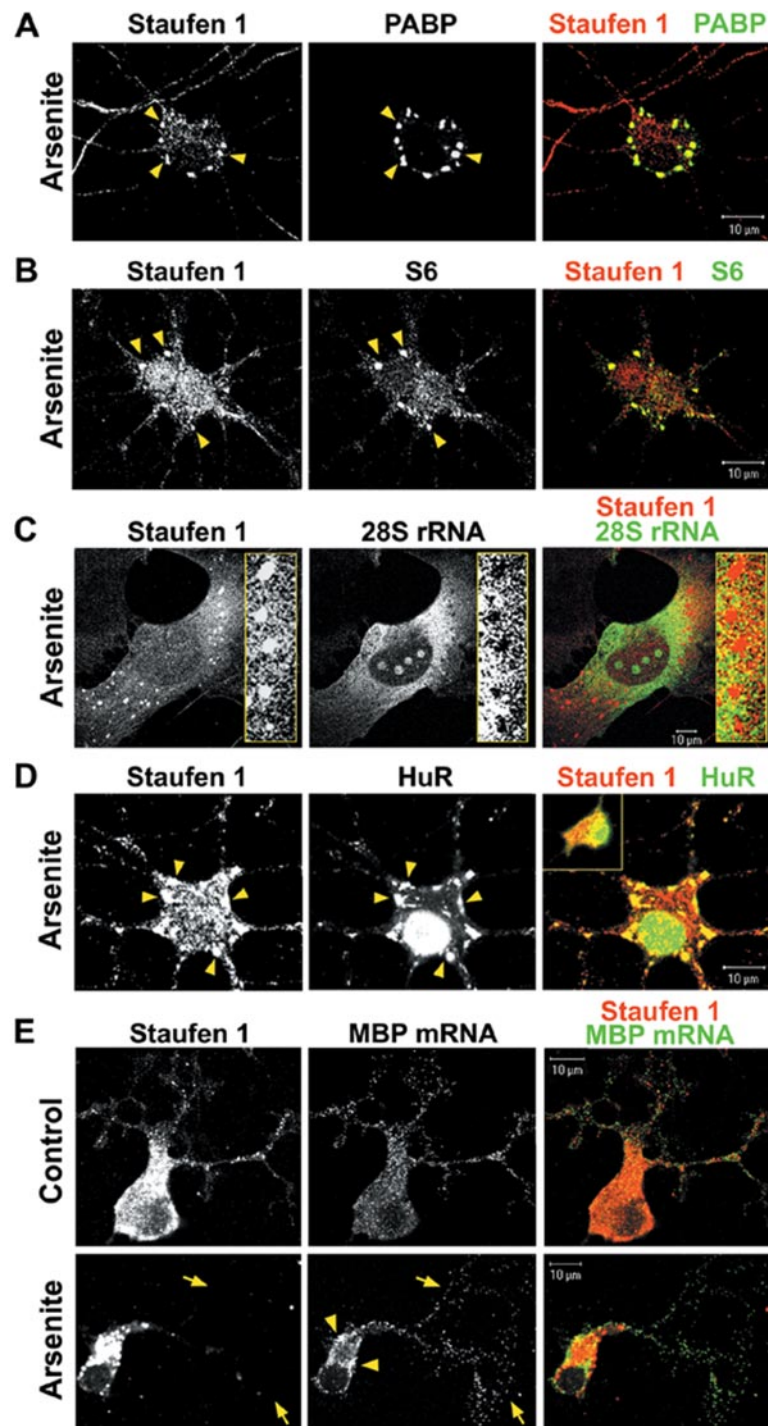


Figure 8. Staufen SGs contain PABP, HuR, and small but no large ribosomal subunits. (A) Staufen 1 strictly colocalizes with PABP in clusters located at the cell body and branching points after 1-h treatment with 0.5 mM arsenite. (B) Staufen and S6 colocalizes in SGs. (C) Staufen SGs exclude large ribosomal subunits. A primary fibroblast is depicted, the inset showing a perinuclear array of SGs at higher magnification. (D) Most of Staufen SGs contain HuR (arrowheads), which is restricted to the cell nucleus in untreated cells (D, inset). (E) On arsenite-induced stress, MBP mRNA partially coalesces into perinuclear aggregates (arrowheads) that do not overlap with Staufen SGs. At the cell processes, MBP mRNA displays the typical fine granular pattern (arrows).

chose to induce SG formation by inhibiting translation. It is known that SG aggregation is triggered by the accumulation of aborted 48S initiation complexes (Anderson and Kedersha, 2002), and thus, we attempted to induce SG formation by blocking translation initiation with edeine, a drug that prevents the entry of the 60S ribosomal subunit. We found that edeine effectively induced SGs, which recruited Staufen 1 and Staufen 2 to a lesser extent, as indicated by the IF pattern (Figure 10, A-C). As expected, these SGs also contained PABP (Figure 10D). Consistently, efficient initiation inhibition was confirmed by

measuring incorporation of radioactive amino acids, which was reduced to 15% relative to nontreated cells (*Materials and Methods*).

The distribution profile of radiolabeled mRNAs after a 6-h chase in the presence of edeine was equivalent to that of control cells (Figure 10E). These observations indicated that the transcripts recently transcribed and exported to the cytoplasm were not recruited into edeine-induced SGs. In addition, their transport and/or diffusion to oligodendrocyte processes was not affected by SG formation or by translation initiation blockage.

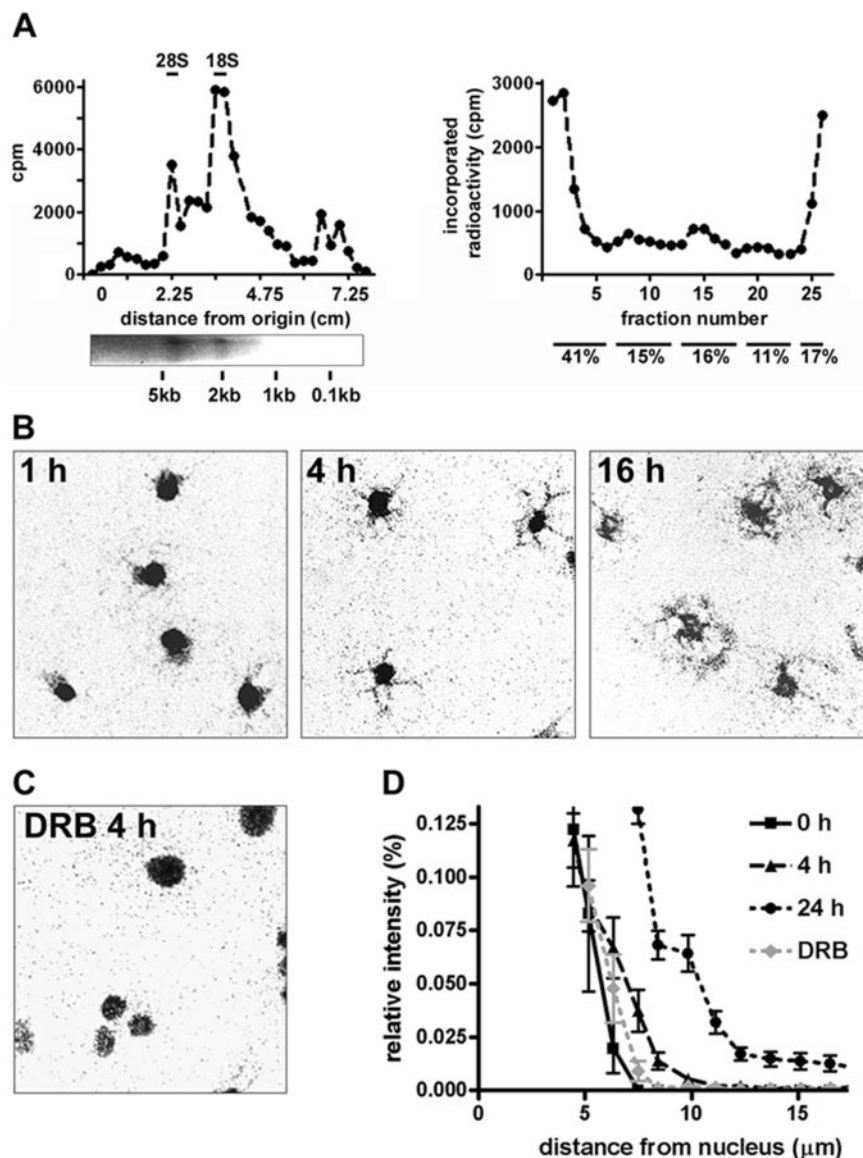


Figure 9. Analysis of cytoplasmic transport of newly synthesized transcripts by pulse and chase radiolabeling. (A) Oligodendrocytes were pulsed with tritiated uridine and chased for 4 h. Left: total RNA was analyzed in a denaturing agarose gel and radioactivity against distance from origin was plotted. Bottom: ethidium bromide staining. The distribution of radiolabel among mRNA (40–50%), rRNA (40–50%), and small RNA (~10%) was similar in three separate experiments. Right: cytosolic extracts were analyzed in 10–30% sucrose gradients. Percentage of incorporated radioactivity in pooled fractions corresponding to free mRNPs (1–6), ribosomal subunits (7–24), and polysomes and large RNPs (19–28), as identified in denaturing agarose gels (unpublished data) is indicated. (B) Oligodendrocytes were pulsed in the absence or presence (C) of DRB, followed by 1-, 4-, or 16-h chase. (D) Radiolabel that accumulated in annular sections (Materials and Methods) relative to whole-cell labeling was plotted against distance from the nucleus at three different chase times. On average, tritiated mRNAs move toward distal oligodendrocyte extensions at 6 $\mu\text{m}/\text{h}$.

DISCUSSION

We have analyzed the expression of Staufen molecules in oligodendrocytes. A 55-kDa Staufen 1 and a 53-kDa Staufen 2 isoforms are expressed in these cells, in agreement with previously reported data in other cell types (Wickham *et al.*, 1999; Kiebler *et al.*, 1999; Brizard *et al.*, 2000; Duchaine *et al.*, 2000, 2002; Monshausen *et al.*, 2001). We found that both, Staufen 1 and Staufen 2 form granules that associate with the cytoskeleton in the tubulin as well as in the actin-rich domains of the myelinating processes. In addition, a fraction of Staufen granules associate with ER membranes, as occurs in neuronal dendrites (Kiebler *et al.*, 1999). The cytoskeletal network and the ER are known platforms for mRNA transport, anchorage, and translation (Kloc *et al.*, 2002; López de Heredia and Jansen, 2003) and thus, it is likely that Staufen granule function depends on these interactions. We have analyzed the distribution of Staufen 1 and Staufen 2 upon oxidative stress and found that both molecules are recruited into stress granules. The parallel analysis of total and of newly synthesized polyadenylated RNA suggests that

Staufen RNPs are linked to the physiology of mRNA molecules engaged in polysomes and unlikely to be connected with that of recently exported mRNA molecules.

Staufen 1, Staufen 2, and the Major Targeted MBP mRNAs form Three Distinct Sets of Granules

Our results demonstrate the existence of at least three distinct kinds of RNA granules located at the myelinating processes, which are selectively loaded with Staufen 1, Staufen 2, or MBP mRNAs. Although Staufen 1 and Staufen 2 granules coexist throughout the oligodendrocyte cytoplasm, they do not colocalize, similarly to what was observed in neurons (Duchaine *et al.*, 2002) and consistently with the finding that Staufen 1 and Staufen 2 particles biochemically isolated from rat brain do not cofractionate (Mallardo *et al.*, 2003). In addition, the frequency of colocalization of Staufen granules with MBP mRNA granules corresponds to a random colocalization ratio (13%), as summarized in the model in Figure 11A. The exclusion of this major transcript from Staufen granules indicates that these proteins have

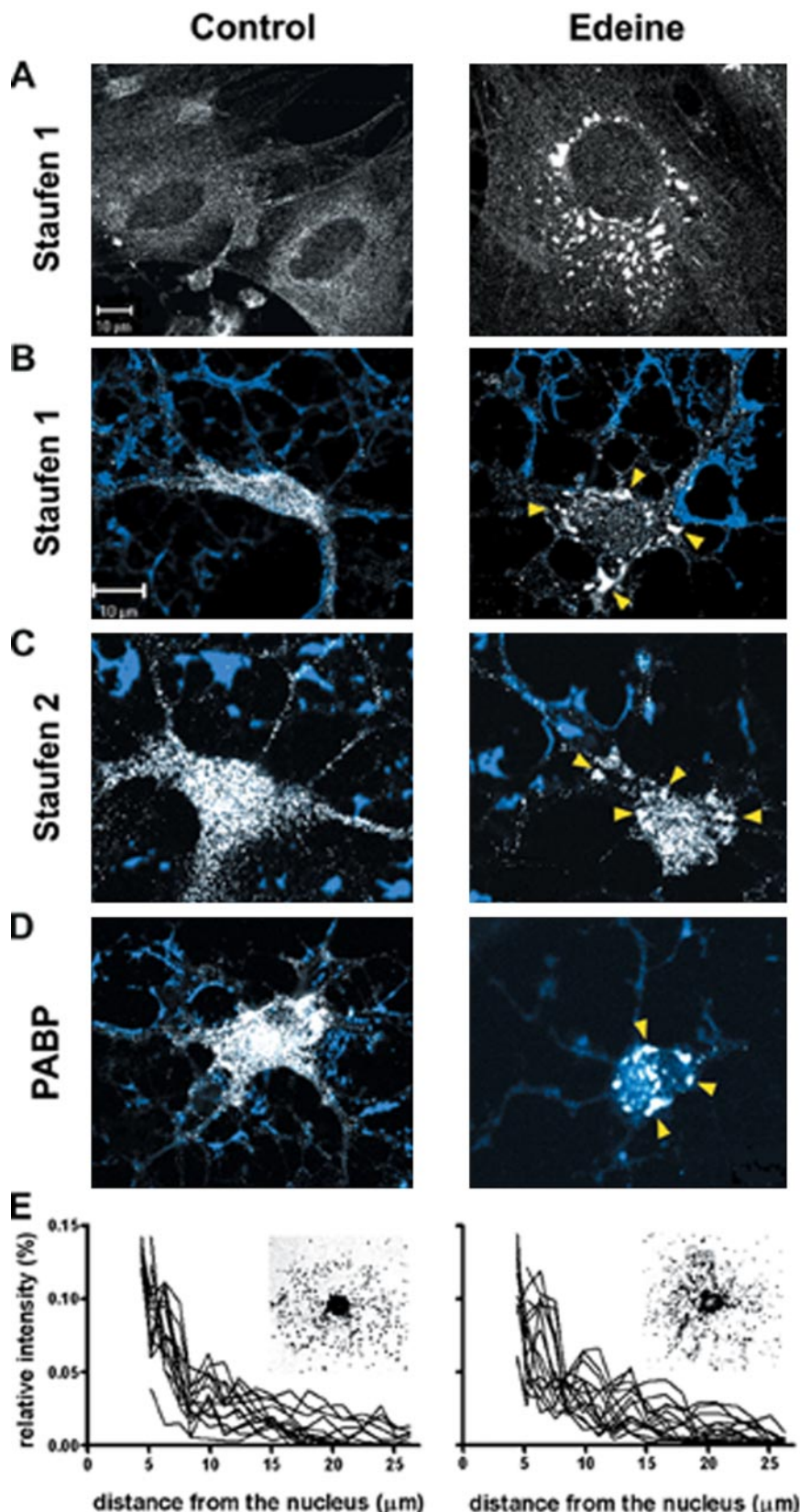


Figure 10. Edeine induces SG formation without affecting the cytoplasmic transport of newly synthesized mRNAs. On protein synthesis blockage by a 6-h treatment with 0.1 mM edeine Staufen 1 (A and B), Staufen 2 (C), and PABP (D) are recruited into SGs. The formation of SGs is observed in primary fibroblasts (A) and oligodendrocytes (B–D, IF for MBP in blue) and affects 36% of the cells at 30 min and 65% at 6 h. (E) Single-cell profiles showing accumulated radiolabeled mRNAs versus distance after a 6-h chase. A similar distribution along the processes is observed in control and treated cells.

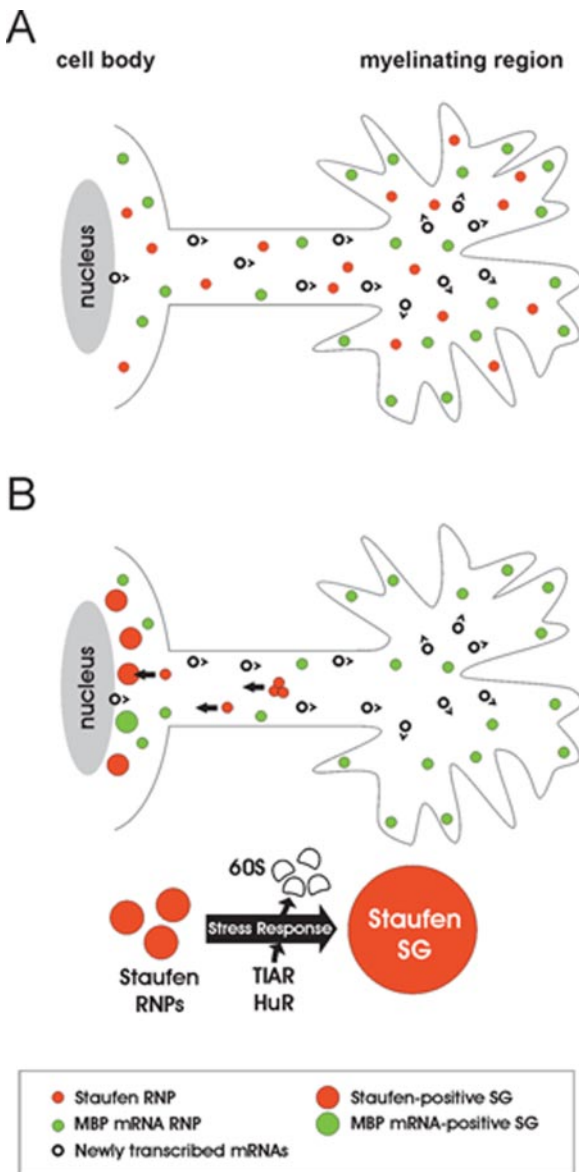


Figure 11. A model for Staufen RNPs and mRNA transport upon normal and stress conditions in myelinating oligodendrocytes. (A) Under normal conditions RNA granules of ~500 nm containing Staufen 1 or Staufen 2 (nondiscriminated in the scheme), or the major MBP mRNAs are present at the cell soma and myelinating extensions. Transport of recently synthesized transcripts toward the myelinating extensions occurs at rates compatible with motor molecule activity (6 μ m/h; Figures 2, 5, and 9). (B) On cellular stress induction, peripheral Staufen granules disappear, whereas perinuclear stress granules containing Staufen 1 and Staufen 2 are formed. SG formation implies the remodeling of normal Staufen RNPs, because large ribosomal subunits are present in normal Staufen granules but are excluded from Staufen stress granules, whereas HuR and TIAR, which normally reside in the nucleus are recruited to SGs (Figures 7 and 8). As in normal conditions, MBP mRNAs are excluded from Staufen SGs. Cytoplasmic transport of newly exported transcripts is not affected by SG formation, as recently synthesized RNA continue traveling toward the cell periphery after induction of SGs by edeine (Figure 10). Our results indicate that SG formation in oligodendrocytes implies the retrograde transport of Staufen RNPs and suggest a role for Staufen RNPs in relocation of mRNAs engaged in polysomes upon external stimuli.

target selectivity and opens the question of which specific myelin messengers are packed into Staufen 1 or Staufen 2 complexes.

Our results, as well as data from related studies that describe similar myelin RNA granules lacking MBP mRNA (Barbarese *et al.*, 1995), strongly suggest the presence of specialized cytoplasmic mRNPs to control protein synthesis at the myelin. This notion is in agreement with the occurrence of the so-called "eukaryotic posttranscriptional operons," which represent mRNPs grouping sets of mRNAs with common features (Keene and Tenenbaum, 2002).

Are the Staufen RNPs translationally active? It is assumed that RNA granules represent silenced units (reviewed in Darnell, 2002; Wickens and Goldstrohm, 2003) and that protein synthesis in SGs is excluded (Kedersha *et al.*, 2000, 2002; Anderson and Kedersha, 2002). In neurons, Staufen 1 was found in granules containing silenced mRNAs as well as ribosomal subunits (Krichevsky and Kosik, 2001). In addition, the presence of the BC1 RNA, a noncoding RNA that mediates the silencing of a number of mRNAs (Zalfa *et al.*, 2003), was demonstrated in neuronal Staufen 1 particles (Ohashi *et al.*, 2002; Mallardo *et al.*, 2003). Therefore, the association of Staufen 1 and Staufen 2 with polysomes observed in oligodendrocytes (this study) and in other cell systems (Kiebler *et al.*, 1999; Marion *et al.*, 1999; Duchaine *et al.*, 2002; Luo *et al.*, 2002) is puzzling, because most polysomes are thought to be actively translating. Nevertheless, mechanisms for mRNA repression were described, in which the mRNA molecules are found in stalled—yet puromycin sensitive—polysomes that do not produce polypeptides (Clark *et al.*, 2000, Ruegsegger *et al.*, 2001). The presence of translationally repressed messengers in myelin Staufen granules remains to be confirmed.

Staufen as a Novel Component of Stress Granules

Stress granules are dynamic structures thought to transiently harbor housekeeping mRNAs when translation is aborted because of stress or drug-induced polysome disruption (Kedersha *et al.*, 2000, 2002; Anderson and Kedersha, 2002). We found that upon edeine or puromycin treatment or upon induction of oxidative stress, Staufen molecules are recruited into SGs. These SGs are located at the cell body and concentrate most of Staufen 1, Staufen 2, and PABP signal when the effect is maximum. Remarkably, as described above for normal RNA granules, the presence of Staufen 1 and MBP mRNA in SGs is mutually exclusive. However, our results indicate that the stress-induced Staufen accretions do not result simply from the clustering of preexisting granules. Instead, a profound remodeling of Staufen granules upon stress is assumed, because 60S ribosomal subunits are present in normal granules and absent from Staufen-containing SGs (Figure 11B). In addition, TIAR and HuR, which normally reside inside the nucleus, are recruited into these structures, further confirming their identity as stress granules.

Our results indicate that Staufen 1 and Staufen 2 are novel and ubiquitous SG components. In addition to the data in primary oligodendrocytes, astrocytes, and fibroblasts, we have confirmed the presence of endogenous and transfected Staufen 1 and Staufen 2 in SGs in several different cell lines (Martinez Tosar and Boccaccio, unpublished observations). Considering the variety of functions thought to occur in SGs—namely mRNA recruitment, silencing, stabilization, and degradation—a relatively reduced number of component RNA-binding proteins were described so far (Gallouzi *et al.*, 2000; Anderson and Kedersha, 2002; Mazroui *et al.*, 2002; Tourrière *et al.*, 2003; Stoecklin *et al.*, 2004). How

Staufen molecules may contribute to stress granule structure, function or dynamics is unknown. Given their ability to form granules by binding to multiple RNA targets and oligomerization via the dsRBDs (Ferrandon *et al.*, 1994; 1997; Micklem *et al.*, 2000; Duchaine *et al.*, 2000), one possibility is that Staufen molecules mediate SG assembly or stability. Moreover, stress granules do not form in the absence of microtubules (Loschi and Boccaccio, unpublished results; Ivanov *et al.*, 2003), suggesting the participation of tubulin-dependent motors to gather the otherwise disperse RNPs. Of relevance, fly Staufen (Micklem *et al.*, 2000), mammalian Staufen (Tang *et al.*, 2001; Ohashi *et al.*, 2002; Mallardo *et al.*, 2003; Brendel *et al.*, 2004; Kanai *et al.*, 2004; Villacé *et al.*, 2004), and *Xenopus* Staufen (Yoon and Mowry, 2004) are known to interact with cellular motors, allowing RNP movement along microtubules. Thus, Staufen molecules may mediate the recruitment of the molecular motors required for SG aggregation.

This study, together with previous reports, supports the notion that SGs and normal RNA granules share component RNA-binding proteins. It has been shown that FMRP and ELAV proteins—two RNA binding proteins present in neuronal RNA granules—similarly redistribute into larger aggregates upon heat shock or puromycin treatment (Antic and Keene, 1998; Mazroui *et al.*, 2002). More recently, the RNA-binding protein SMN, which forms granules in neurons (Zhang *et al.*, 2003), was shown to be present in cytoplasmic granules containing TIAR and TIA-1 in both normal and stress conditions (Hua and Zhou, 2004). Thus, an interconversion between SGs and normal RNA granules exists, adding more elements to the dynamic equilibrium thought to occur between different cytosolic ribonucleoparticles: polysomes and normal mRNA granules (Krichevsky and Kosik, 2001), and polysomes and stress granules (Anderson and Kedersha, 2002).

Staufen RNPs in Early and Late mRNA Localization Events

We have analyzed the distribution of Staufen molecules in normal and stress granules in comparison with the subcellular distribution of polyadenylated RNA, visualized by staining for the surrogate marker PABP, and with the localization of recently transcribed mRNA molecules, labeled by metabolic incorporation of tritiated uridine. Our results are consistent with previous work carried out in neurons (Köhrmann *et al.*, 1999; Tang *et al.*, 2001) and suggest that Staufen RNPs participate in late positioning or repositioning of polysomal mRNAs. Simultaneously, as summarized in Figure 11B, our data suggest that the role of Staufen RNPs in early mRNA transport to the oligodendrocyte periphery is nonessential, as the abundance of young mRNA molecules at this cellular compartment was not affected by the recruitment of Staufen 1 (and Staufen 2 to a lesser extent) into edeine-induced SGs. Of course, an effect on the movement of minor mRNA species cannot be excluded. Relevantly, *Drosophila* Staufen is involved in the late localization stages of *bicoid* and *oskar* mRNAs and is not required for the initial transport events of these messengers (reviewed in Lasko, 1999; Kiebler and Desgroseillers, 2000). Furthermore, the *Xenopus* Staufen homologue is incorporated to transport ribonucleoparticles once in the cytoplasm (Kress *et al.*, 2004), where is required for mRNA localization to the oocyte vegetal pole (Yoon and Mowry, 2004). Altogether these data support a role for Staufen molecules in late, cytoplasmic steps of mRNA transport throughout evolution.

Our finding that edeine does not affect mRNA transport to the myelinating region is consistent with the notion that

translation is not required for transport (Kleinman *et al.*, 1993; Palacios and St Johnston, 2001; Kloc *et al.*, 2002). In addition, our results indicate that in contrast to most polyadenylated RNA, recently transcribed mRNA molecules were not massively recruited into SGs upon edeine treatment. This suggests that young mRNA molecules are not engaged in stress-sensitive polysomes. In addition, because edeine blocks normal initiation, the recently exported mRNAs are likely transported before their first round of translation. It is conceivable that before the onset of productive translation, mRNA molecules need to adjust their position in the cytoplasm, as they have to pass the quality control known as non-sense-mediated decay, which has been proposed to act also at early stages (Ishigaki *et al.*, 2001; Maquat and Carmichael, 2001). Accordingly, it has been recently shown that protein factors involved in NMD are required for mRNA localization (Palacios *et al.*, 2004).

We speculate that Staufen RNPs participate in a late stage of mRNA localization, involving the final positioning or repositioning of mRNAs likely associated to polysomes. Several lines of evidence support this notion. First, RNA granules containing Staufen 1 show microtubule-dependent anterograde as well as retrograde movement in neurons (Köhrmann *et al.*, 1999). Second, Staufen particles contain ribosome subunits and are associated to polysomes (this work; Kiebler *et al.*, 1999; Duchaine *et al.*, 2002; Luo *et al.*, 2002; Brendel *et al.*, 2004; Villacé *et al.*, 2004; Yoon and Mowry, 2004). Third, total RNA distribution in neurons correlates with the localization of overexpressed Staufen 2 constructs (Tang *et al.*, 2001). Finally, upon cellular stress induction, ribosome-containing Staufen 1 and Staufen 2 particles redistribute together with poly(A) RNA in several cell types in a microtubule-dependent manner (this work).

Given their profound and selective remodeling upon stress, we predict that the localization of Staufen RNPs in glial cells will respond to extracellular stimuli, similarly to the redistribution of mRNPs and polysomes in fibroblasts and neurons prompted by growth factors, synaptic stimulation, or integrin signaling (Knowles and Kosik, 1997; Chircurel *et al.*, 1998; Zhang *et al.*, 2001; Ostroff *et al.*, 2002; Tiruchinapalli *et al.*, 2003). The mechanism by which Staufen RNPs participate in the repositioning of polysomal mRNAs as well as their relevance in the assembly or stability of stress granules are open issues that remain to be investigated.

ACKNOWLEDGMENTS

We thank Ayelén Bulloj, Cornelia Brendel, María Verónica Baez, and the laboratory of Fernando Goldbaum (Fundación Instituto Leloir) for help in riboprobe and antibody preparations. We are also grateful to Dr J. Ortín (Centro Nacional de Biología, Spain) and Dr. M. Kiebler (Max Planck Institute, Germany) for anti-Staufen antibodies; Dr. E. Mohr (University of Hamburg, Germany) for anti-PABP serum; Dr. J. Steitz (HHMI-Yale University, New Haven, CT) for Y10B and anti-HuR monoclonal antibodies, and Dr. I. Algranati (Fundación Instituto Leloir) for providing edeine. This work was supported by grants from the Agencia Nacional de Promoción Científica y Tecnológica (PICT 01-08691) (Argentina), the Third World Academy of Sciences, National Institutes of Health, (IR03 TW 006037-01A1), and the Wadsworth Foundation (USA) to G.L.B., from Fundación para la Lucha contra las Enfermedades Neurológicas de la Infancia to J.C. and by a grant from Fundación Antorchas (14022/93) (Argentina) and DAAD (Germany) to G.L.B. and S.K. G.L.B. is a member of the Consejo Nacional de Investigaciones Científicas y Tecnológicas, and M.G.T. and L.J.M.T. are recipients of a fellowship from CONICET and of the Luis Federico Leloir 2002 award, respectively.

REFERENCES

- Ainger, K., Avossa, D., Diana, A. S., Barry, C., Barbarese, E., and Carson, J. H. (1997). Transport and localization elements in myelin basic protein mRNA. *J. Cell Biol.* 138, 1077–1087.

- Anderson, P., and Kedersha, N. (2002). Stressful initiations. *J. Cell Sci.* **115**, 3227–3234.
- Antic, D., and Keene, J. D. (1998). Messenger ribonucleoprotein complexes containing human ELAV proteins: interactions with cytoskeleton and translational apparatus. *J. Cell Sci.* **111**, 183–197.
- Barbarese, E., Brumwell, C., Kwon, S., Cui, H., and Carson, J. H. (1999). RNA on the road to myelin. *J. Neurocytol.* **28**, 263–270.
- Barbarese, E., Koppel, D. E., Deutscher, M. P., Smith, C. L., Ainger, K., Morgan, F., and Carson, J. H. (1995). Protein translation components are colocalized in granules in oligodendrocytes. *J. Cell Sci.* **108**, 2781–2790.
- Barry, C., Pearson, C., and Barbarese, E. (1996). Morphological organization of oligodendrocyte processes during development in culture and in vivo. *Dev. Neurosci.* **18**, 233–242.
- Brendel, C., Rehbein, M., Kreienkamp, H. J., Buck, F., Richter, D., and Kindler, S. (2004). Characterization of Staufen 1 ribonucleoprotein complexes. *Biochem. J.* **383**, 1–8.
- Brizard, F., Luo, M., and Desgroseillers, L. (2000). Genomic organization of the human and mouse stau genes DNA. *Cell. Biol.* **19**, 331–339.
- Brophy, P. J., Boccaccio, G. L., and Colman, D. R. (1993). The distribution of myelin basic protein mRNAs within myelinating oligodendrocytes. *Trends Neurosci.* **16**, 515–521.
- Carson, J. H., Cui, H., and Barbarese, E. (2001). The balance of power in RNA trafficking. *Curr. Opin. Neurobiol.* **11**, 558–563.
- Carson, J. H., Kwon, S., and Barbarese, E. (1998). RNA trafficking in myelinating cells. *Curr. Opin. Neurobiol.* **8**, 607–612.
- Casaccia-Bonelli, P., Aibel, L., and Chao, M. V. (1996). Central glia and neuronal populations display differential sensitivity to ceramide-dependent cell death. *J. Neurosci. Res.* **43**, 382–389.
- Chicurel, M. E., Singer, R. H., Meyer, C. J., and Ingber, D. E. (1998). Integrin binding and mechanical tension induce movement of mRNA and ribosomes to focal adhesions. *Nature* **392**, 730–733.
- Clark, I. E., Wyckoff, D., and Gavis, E. R. (2000). Synthesis of the posterior determinant Nanos is spatially restricted by a novel cotranslational regulatory mechanism. *Curr. Biol.* **10**(20), 1311–1314.
- Darnell, R. B. (2002). RNA logic in time and space. *Cell* **110**, 545–550.
- Dubnau, J. et al. (2003). The staufen/pumilio pathway is involved in *Drosophila* long-term memory. *Curr. Biol.* **13**, 286–296.
- Duchaine, T., Wang, H. J., Luo, M., Steinberg, S. V., Nabi, I. R., and DesGroseillers, L. (2000). A novel murine Staufen isoform modulates the RNA content of Staufen complexes. *Mol. Cell. Biol.* **20**, 5592–5601.
- Duchaine, T. F., Hemraj, I., Furic, L., Deitinghoff, A., Kiebler, M. A., and DesGroseillers, L. (2002). Staufen2 isoforms localize to the somatodendritic domain of neurons and interact with different organelles. *J. Cell Sci.* **115**, 3285–3295.
- Ferrandon, D., Elphick, L., Nusslein-Volhard, C., and St. Johnston, D. (1994). Staufen protein associates with the 3'UTR of bicoid mRNA to form particles that move in a microtubule-dependent manner. *Cell* **79**, 1221–1232.
- Ferrandon, D., Koch, I., Westhof, E., and Nusslein-Volhard, C. (1997). RNA-RNA interaction is required for the formation of specific bicoid mRNA 3' UTR-Staufen ribonucleoprotein particles. *EMBO J.* **16**, 1751–1758.
- Gallouzi, I. E., Brennan, C. M., Stenberg, M. G., Swanson, M. S., Eversole, A., Maizels, N., and Steitz, J. A. (2000). HuR binding to cytoplasmic mRNA is perturbed by heat shock. *Proc. Natl. Acad. Sci. USA* **97**, 3073–3078.
- Garden, G. A., Hartlage-Rubsamen, M., Rubel, E. W., and Bothwell, M. A. (1995). Protein masking of a ribosomal RNA epitope is an early event in afferent deprivation-induced neuronal death. *Mol. Cell. Neurosci.* **6**, 293–310.
- Gould, R. M., Freund, C. M., Palmer, F., and Feinstein, D. L. (2000). Messenger RNAs located in myelin sheath assembly sites. *J. Neurochem.* **75**, 1834–1844.
- Hua, Y., and Zhou, J. (2004). Survival motor neuron protein facilitates assembly of stress granules. *FEBS Lett.* **572**, 69–74.
- Ishigaki, Y., Li, X., Serin, G., and Maquat, L. E. (2001). Evidence for a pioneer round of mRNA translation: mRNAs subject to nonsense-mediated decay in mammalian cells are bound by CBP80 and CBP20. *Cell* **106**, 607–617.
- Ivanov, P. A., Chudinova, E. M., and Nadezhina, E. S. (2003). Disruption of microtubules inhibits cytoplasmic ribonucleoprotein stress granule formation. *Exp. Cell. Res.* **290**, 227–233.
- Jackson, D. A., Iborra, F. J., Manders, E. M., and Cook, P. R. (1998). Numbers and organization of RNA polymerases, nascent transcripts, and transcription units in HeLa nuclei. *Mol. Biol. Cell* **9**, 1523–1536.
- Jacobs, E. Y., Frey, M. R., Wu, W., Ingledue, T. C., Gebuhr, T. C., Gao, L., Marzluff, W. F., and Matera, A. G. (1999). Coiled bodies preferentially associate with U4, U11, and U12 small nuclear RNA genes in interphase HeLa cells but not with U6 and U7 genes. *Mol. Biol. Cell* **10**, 1653–1663.
- Kanai, Y., Dohmae, N., and Hirokawa, N. (2004). Kinesin transports RNA; isolation and characterization of an RNA-transferring granule. *Neuron* **43**, 513–525.
- Kedersha, N., Chen, S., Gilks, N., Li, W., Miller, I. J., Stahl, J., and Anderson, P. (2002). Evidence that ternary complex (eIF2-GTP-tRNA(i)Met)-deficient preinitiation complexes are core constituents of mammalian stress granules. *Mol. Biol. Cell* **13**, 195–210.
- Keene, J. D., Cho, M. R., Li, W., Yacono, P. W., Chen, S., Gilks, N., Golan, D. E., and Anderson, P. (2000). Dynamic shuttling of TIA-1 accompanies the recruitment of mRNA to mammalian stress granules. *J. Cell Biol.* **151**, 1257–1268.
- Keene, J. D., and Tenenbaum, S. A. (2002). Eukaryotic mRNPs may represent posttranscriptional operons. *Mol. Cell* **9**, 1161–1167.
- Kiebler, M. A., and Desgroseillers, L. (2000). Molecular insights into mRNA transport and local translation in the mammalian nervous system. *Neuron* **25**, 19–28.
- Kiebler, M. A., Hemraj, I., Verkade, P., Kohrmann, M., Fortes, P., Marion, R. M., Ortín, J., and Dotti, C. G. (1999). The mammalian Staufen protein localizes to the somatodendritic domain of cultured hippocampal neurons: implications for its involvement in mRNA transport. *J. Neurosci.* **19**, 288–297.
- Kleinman, R., Banker, G., and Steward, O. (1993). Inhibition of protein synthesis alters the subcellular distribution of mRNA in neurons but does not prevent dendritic transport of RNA. *Proc. Natl. Acad. Sci. USA* **90**, 11192–11196.
- Kloc, M., Zearfoss, N.R., and Etkin, L.D. (2002). Mechanisms of subcellular mRNA localization. *Cell* **108**, 533–544.
- Knowles, R.B., and Kosik, K.S. (1997). Neurotrophin-3 signals redistribute RNA in neurons. *Proc. Natl. Acad. Sci. USA* **94**, 14804–14808.
- Köhrrmann, M., Luo, M., Kaether, C., DesGroseillers, L., Dotti, C. G., and Kiebler, M. A. (1999). Microtubule-dependent recruitment of Staufen-green fluorescent protein into large RNA-containing granules and subsequent dendritic transport in living hippocampal neurons. *Mol. Biol. Cell* **10**, 2945–2955.
- Kress, T. L., Yoon, Y. J., and Mowry, K. L. (2004). Nuclear RNP complex assembly initiates cytoplasmic RNA localization. *J. Cell Biol.* **165**, 203–211.
- Krichevsky, A. M., and Kosik, K. S. (2001). Neuronal RNA granules: a link between RNA localization and stimulation-dependent translation. *Neuron* **32**, 683–696.
- Lasko, P. (1999). RNA sorting in *Drosophila* oocytes and embryos. *FASEB J.* **13**, 421–433.
- Lerner, E. A., Lerner, M. R., Janeway, C. A., Jr., and Steitz, J. A. (1981). Monoclonal antibodies to nucleic acid-containing cellular constituents: probes for molecular biology and autoimmune disease. *Proc. Natl. Acad. Sci. USA* **78**, 2737–2741.
- López de Heredia, M., and Jansen, R. (2003). mRNA localization and the cytoskeleton. *Curr. Opin. Cell Biol.* **16**, 1–6.
- Luo, M., Duchaine, T. F., and DesGroseillers, L. (2002). Molecular mapping of the determinants involved in human Staufen/ribosome association. *Biochem. J.* **365**, 817–824.
- Macchi, P. et al. (2003). Barentsz, a new component of the Staufen-containing ribonucleoprotein particles in mammalian cells, interacts with Staufen in an RNA-dependent manner. *J. Neurosci.* **23**, 5778–5788.
- Mallardo, M., Deitinghoff, A., Muller, J., Goetze, B., Macchi, P., Peters, C., and Kiebler, M. A. (2003). Isolation and characterization of Staufen-containing ribonucleoprotein particles from rat brain. *Proc. Natl. Acad. Sci. USA* **100**, 2100–2105.
- Maquat, L. E., and Carmichael, G. G. (2001). Quality control of mRNA function. *Cell* **104**, 173–176.
- Marion, R. M., Fortes, P., Beloso, A., Dotti, C., and Ortín, J. (1999). A human sequence homologue of Staufen is an RNA-binding protein that is associated with polysomes and localizes to the rough endoplasmic reticulum. *Mol. Cell. Biol.* **19**, 2212–2219.
- Mathisen, P. M., Johnson, J. M., and Kawezak, J. A. (1997). Stabilization of myelin mRNAs as measured in a brain slice system. *J. Neurosci. Res.* **50**, 1030–1039.
- Mazroui, R., Huot, M. E., Tremblay, S., Filion, C., Labelle, Y., and Khandjian, E. W. (2002). Trapping of messenger RNA by Fragile X Mental Retardation protein into cytoplasmic granules induces translation repression. *Hum. Mol. Genet.* **11**, 3007–30017.

- McCarthy, K. D., and de Vellis, J. (1980). Preparation of separate astroglial and oligodendroglial cell cultures from rat cerebral tissue. *J. Cell Biol.* 85, 890–902.
- Micklem, D. R., Adams, J., Grunert, S., and St. Johnston, D. (2000). Distinct roles of two conserved Staufen domains in oskar mRNA localization and translation. *EMBO J.* 19, 1366–1377.
- Monshausen, M., Putz, U., Rehbein, M., Schweizer, M., DesGroseillers, L., Kuhl, D., Richter, D., and Kindler, S. (2001). Two rat brain staufen isoforms differentially bind RNA. *J. Neurochem.* 76, 155–165.
- Monshausen, M., Rehbein, M., Richter, D., and Kindler, S. (2002). The RNA-binding protein Staufen from rat brain interacts with protein phosphatase-1. *J. Neurochem.* 81, 557–564.
- Ohashi, S., Koike, K., Omori, A., Ichinose, S., Ohara, S., Kobayashi, S., Sato, T.A., and Anzai, K. (2002). Identification of mRNA/protein (mRNP) complexes containing Puralph, mStaufen, fragile X protein, and myosin Va and their association with rough endoplasmic reticulum equipped with a kinesin motor. *J. Biol. Chem.* 277, 37804–37810.
- Ostroff, L. E., Fiala, J.C., Allwardt, B., and Harris, K. M. (2002). Polyribosomes redistribute from dendritic shafts into spines with enlarged synapses during LTP in developing rat hippocampal slices. *Neuron* 35, 535–545.
- Palacios, I. M., and St. Johnston, D. (2001). Getting the message across: the intracellular localization of mRNAs in higher eukaryotes. *Annu. Rev. Cell. Dev. Biol.* 17, 569–614.
- Palacios, I. M., Gatfield, D., St. Johnston, D., and Izaurralde, E. (2004). An eIF4AIII-containing complex required for mRNA localization and nonsense-mediated mRNA decay. *Nature* 427, 753–757.
- Ruegsegger, U., Leber, J. H., and Walter, P. (2001). Block of HAC1 mRNA translation by long-range base pairing is released by cytoplasmic splicing upon induction of the unfolded protein response. *Cell* 107, 103–114.
- Saugaitis, S. M., Smith, P. R., and Colman, D. R. (1990). Expression of myelin basic protein isoforms in nonglial cells. *J. Cell Biol.* 110, 1719–1727.
- Stoecklin, G., Stubbs, T., Kedersha, N., Wax, S., Rigby, W. F., Blackwell, T. K., and Anderson, P. (2004). MK2-induced tristetraprolin:14-3-3 complexes prevent stress granule association and ARE-mRNA decay. *EMBO J.* 23, 1313–1324.
- Suzumura, A., Bhat, S., Eccleston, P. A., Lisak, R. P., and Silberberg, D. H. (1984). The isolation and long-term culture of oligodendrocytes from newborn mouse brain. *Brain Res.* 324, 379–383.
- Tang, S. J., Meulemans, D., Vazquez, L., Colaco, N., and Schuman, E. (2001). A role for a rat homolog of staufen in the transport of RNA to neuronal dendrites. *Neuron* 32, 463–475.
- Tiruchinapalli, D. M., Oleynikov, Y., Kelic, S., Shenoy, S. M., Hartley, A., Stanton, P. K., Singer, R. H., and Bassell, G. J. (2003). Activity-dependent trafficking and dynamic localization of zipcode-binding protein 1 and beta-actin mRNA in dendrites and spines of hippocampal neurons. *J. Neurosci.* 23, 3251–3261.
- Tourrière, H., Chebli, K., Zekri, L., Courselaud, B., Blanchard, J. M., Bertrand, E., and Tazi, J. (2003). The RasGAP-associated endoribonuclease G3BP assembles stress granules. *J. Cell Biol.* 160, 823–831.
- Villacé, P., Marion, R. M., and Ortín, J. (2004). The composition of Staufen-containing RNA granules from human cells indicates their role in the regulated transport and translation of messenger RNAs. *Nucleic Acids Res.* 32, 2411–2420.
- Wickens, M., and Goldstrohm, A. (2003). A place to die, a place to sleep. *Science* 300, 753–755.
- Wickham, L., Duchaine, T., Luo, M., Nabi, I. R., and DesGroseillers, L. (1999). Mammalian Staufen is a double-stranded RNA and Tubulin-binding protein which localizes to the rough endoplasmic reticulum. *Mol. Cell. Biol.* 19, 2220–2230.
- Yoon, Y. J., and Mowry, K. L. (2004). *Xenopus* Staufen is a component of a ribonucleoprotein complex containing Vg1 RNA and kinesin. *Development* 131, 3035–3045.
- Zalfa, F., Giorgi, M., Primerano, B., Moro, A., Di Penta, A., Reis, S., Oostra, B., and Bagni, C. (2003). The fragile X syndrome protein FMRP associates with BC1 RNA and regulates the translation of specific mRNAs at synapses. *Cell* 112, 317–327.
- Zhang, H. L., Eom, T., Oleynikov, Y., Shenoy, S. M., Liebelt, D. A., Dictenberg, J. B., Singer, R. H., and Bassell, G. J. (2001). Neurotrophin-induced transport of a beta-actin mRNP complex increases beta-actin levels and stimulates growth cone motility. *Neuron* 31, 261–275.
- Zhang, H. L., Pan, F., Hong, D., Shenoy, S. M., Singer, R. H., and Bassell, G. J. (2003). Active transport of the survival motor neuron protein and the role of exon-7 in cytoplasmic localization. *J. Neurosci.* 23, 6627–6637.